LAGRANGIAN METHODS FOR CLIMATOLOGICAL ANALYSIS OF REGIONAL ATMOSPHERIC TRANSPORT WITH AN EMPHASIS ON TEXAS OZONE EXCEEDANCES

A Thesis

by

DARIELLE DEXHEIMER

Submitted to the Office of Graduate Studies of
Texas A&M University
in partial fulfillment of the requirements for the degree of

MASTER OF SCIENCE

August 2004

Major Subject: Atmospheric Sciences

LAGRANGIAN METHODS FOR CLIMATOLOGICAL ANALYSIS OF REGIONAL ATMOSPHERIC TRANSPORT WITH AN EMPHASIS ON TEXAS OZONE EXCEEDANCES

A Thesis

by

DARIELLE DEXHEIMER

Submitted to Texas A&M University
in partial fulfillment of the requirements
for the degree of

MASTER OF SCIENCE

Approved as to style and content by:

Kenneth P. Bowman (Chair of Committee)	Don Collins (Member)
Steven DiMarco (Member)	Richard Orville (Head of Department)

August 2004

Major Subject: Atmospheric Sciences

ABSTRACT

Lagrangian Methods for Climatological Analysis of Regional Atmospheric Transport With an Emphasis on Texas Ozone Exceedances. (August 2004)

Darielle Dexheimer, B.S., Texas A&M University

Chair of Advisory Committee: Dr. Kenneth P. Bowman

A quantitative climatology of atmospheric transport in Texas is developed using previously described Lagrangian trajectory methods (Rogers and Bowman, 2001; Bowman and Carrie, 2002). The trajectories are computed using winds from 1979–2001 from the National Center for Environmental Prediction (NCEP) Reanalysis Project data set.

Probability distributions are created for particle transport using trajectories from urban areas, making six-hourly particle distributions available from four urban areas in Texas. These probability distributions represent a quantitative understanding of regional air transport.

Time-dependent Green's functions are calculated given initial conditions such as urban areas weighted with respect to population. The Green's functions describe how air from urban areas is transported through the atmosphere as a function of time.

Summertime backward Lagrangian trajectories initialized at 5 Texas Commission on Environmental Quality (TCEQ) monitoring stations are grouped according to the ozone value recorded at the station at the initialization time of the trajectory. The directions of the trajectories in each group are used to determine the relationship between the transport characteristics of the circulation over Texas and regional-scale observations of pollutants.

Synoptic conditions occurring at the time of summertime ozone exceedances at the 5 TCEQ stations are investigated in order to resolve what conditions are likely to coincide with ozone exceedances.

TABLE OF CONTENTS

CHAPTER Page

LIST OF TABLES

LIST OF FIGURES

FIGURE Page

FIGURE Page

FIGURE Page

CHAPTER I

INTRODUCTION

Among the unfortunate consequences of increasing population and economic growth in many areas of the world are serious urban and regional air-quality problems. These problems can result from both local emissions and from the transport of pollutants from outside the local area. As a result, understanding regional atmospheric transport is crucial to determining the relationship between source locations and local air quality.

Previous studies have been conducted of regional-scale pollution events (Rogers and Bowman, 2001; Peppler, 2000). Rogers and Bowman (Rogers and Bowman, 2001) investigated the unusual transport of biomass-burning smoke from Mexico and Central America to the United States during the spring and early summer of 1998. They found that, at that time of year, transport from southern Mexico and northern Central America alternates between northward flow toward the United States and westward flow into the Pacific basin. During the spring of 1998, drought and widespread agricultural burning led to unusually large smoke production. During May 1998, episodes of northward flow were more common than during other recent years, and at times large amounts of smoke were transported into the central and eastern United States. The heavy amounts of smoke observed in the southeastern United States at that time can be attributed both to unusual smoke production and to abnormally strong northward transport.

This study describes a quantitative method to characterize the climatological regional-scale transport by relating kinematic particle trajectories to the solutions of the mass

---

This thesis follows the style of *Journal of Applied Meteorology*.

conservation equation for a passive trace substance. The climatology can be used, among other things, to determine the likelihood that a region would be influenced by transport from particular source areas.

From 1997-2002 there were over 100 hours a year when one-hour ozone levels met or exceeded the federal standard of 125 ppb at monitoring stations in Texas. One-hour ozone values greater than or equal to 125 ppb are known by the EPA to cause severe respiratory symptoms and impair breathing in sensitive groups. Additionally, if an area exceeds the federal ozone standard four times in three years and fails to develop or implement a state plan to comply with the standard it is subject to the loss of federal highway funds, limits on industrial expansion, and the loss of federal Air Pollution Control Program grant funds. The need to understand what meteorological conditions are conducive to ozone exceedances in Texas is evident for both health and financial reasons.

A previous study of the meteorology behind ozone exceedances in the Houston area was conducted during the Texas Air Quality Study of 2000 (Senff *et al.* , 2002). The occurrence of widespread ozone exceedances and high peak ozone values was linked to two meteorological factors, light-wind conditions during midday and the afternoon sea breeze. Light winds allowed a buildup of plumes over the source regions, while the sea breeze transported pollutants back inland after they moved offshore during the morning. Subtle changes in the onset, strength, and direction of the sea breeze resulted in significant differences in the peak values and distribution of ozone.

This study investigates the meteorological conditions present when ozone exceedances occur at selected monitoring stations in Texas. An understanding of these conditions will allow more accurate forecasting of high ozone events, and will assist in the formation of a climatology of Texas ozone exceedances.

CHAPTER II

DATA AND INSTRUMENTS

A. NCEP reanalysis data

In this study, trajectories are computed using three-dimensional winds from the National Center for Environmental Prediction (NCEP) Reanalysis Project data set (Kalnay *et al.* , 1996). These data are used because of their temporal and spatial coverage, quality control, and availability. The reanalysis process uses a uniform global data-assimilation system. Input data for the reanalysis include global rawinsonde data, Comprehensive Ocean-Atmosphere Data Set (COADS) surface marine data, aircraft data, surface and synoptic data, satellite sounder data, and Special Sensing Microwave/Imager (SSM/I)surface wind speeds. The quality and quantity of these data sources varies with time. For this study, data are taken from the 22-year period 1979–2000.

The NCEP reanalysis includes data for temperature, geopotential height, and zonal and meridional wind at 17 pressure levels from 1000 to 10 hPa, and vertical velocity in pressure coordinates at the 12 lowest pressure levels. Data are available on a $2.5^\circ \times 2.5^\circ$ global longitude-latitude grid. The relatively coarse resolution of the model grid for regional-scale analysis is offset by the quality and length of the data record and the uniformity of the assimilation methods. The methods described below can be applied to higher-resolution retrospective data sets as they become available in the future, or to forecast products. Mean climatological geopotential heights are taken from the long-term climatological means, which are based on the 29-year period 1968–1996.

B. Air quality data

The air quality data used includes hourly ozone values from TCEQ Continuous Air Monitoring System (CAMS) stations. At these stations ozone is measured using an ultraviolet (UV) absorbance method where a stable UV source beams through an airstream containing the air sample and an ozone free reference stream. The difference in UV transmission is correlated to the ozone concentration in the sample stream. The atmosphere is sampled every second at the CAMS stations, and every five minutes an average of all the one-second samples collected is taken. Hourly averages are then calculated from these five-minute averages. The TCEQ convention for time-tagging data is the beginning of each hour. Thus, the 9:00 am data is data collected between 9:00 and 10:00 am.

Hourly ozone data from 1997–2000 is available at www.tceq.state.tx.us from over 200 CAMS stations in Texas. From the over 200 CAMS stations, five stations in eastern Texas are chosen for study based on their locations, quality of data, and length of data collection. The locations of these five stations: 1) Fort Worth Northwest C13, 2) Tyler Airport C86, 3) Longview C19, 4) Cypress River C50, and 5) Aldine C8 are shown in Figure 1. Their latitudes and longitudes are given in Table I. Longview and Tyler are small cities with a population of less than 85,000 each. Jefferson, which is near the station Cypress River C50, is a small town with a population of 2200. The three cities are all within 100 km of each other, and are approximately 200 km east of Dallas/Fort Worth and 250 km north of Houston. The other two stations studied, Aldine C8 and Fort Worth Northwest C13, are located approximately 10 km southwest of downtown Houston and 10 km northwest of downtown Fort Worth, respectively. Data has been collected at Aldine C8 and Fort Worth Northwest C13 from January 1, 1979 to the present, at Tyler Airport Relocated C86 from August 2, 1994 to May 16, 2000, at Longview C19 from January 1, 1996 to the present, and

Table I. Latitudes and longitudes of the five selected Continuous Air Monitoring System (CAMS) stations.

Number	Station Name	Latitude	Longitude
1	Fort Worth Northwest C13	32.8058°N	-97.3567°W
2	Tyler Airport C86	32.3580°N	-95.4097°W
3	Longview C19	37.3825°N	-94.7125°W
4	Cypress River C50	32.7428°N	-94.3033°W
5	Aldine C08	29.9011°N	-95.3261°W

at Cypress River C50 from May 1, 1998 to December 31, 2000. The rural sites (Cypress River, Longview, and Tyler Airport were chosen because they are outside the immediate influence of large urban areas.

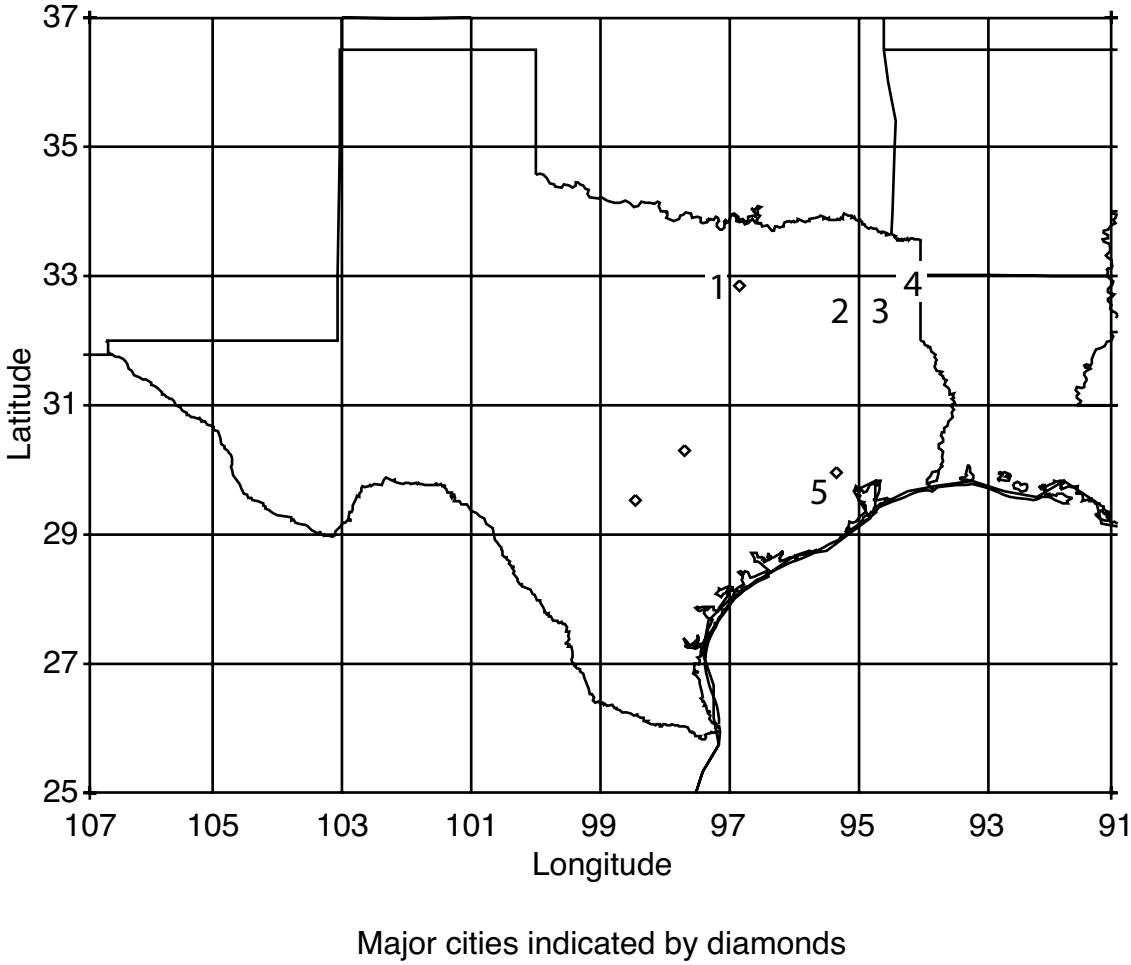

Fig. 1. Locations of five selected Continuous Air Monitoring System (CAMS) stations: 1) Fort Worth Northwest C13, 2) Tyler Airport C86, 3) Longview C19, 4) Cypress River C50, and 5) Aldine C8.

CHAPTER III

METHODS

A. Green's function method

In order to characterize the climatological transport circulation, we use particle trajectories to estimate the Green's functions of the mass continuity equation for a conserved trace substance

$$\frac{\partial s}{\partial t} + \mathbf{v} \cdot \nabla s = 0, \qquad s(\mathbf{x}, t_0) = s_0(\mathbf{x}), \tag{3.1}$$

where $\mathbf{x}$ is position, t is time, s is the mass mixing ratio of the trace substance, $\mathbf{v}$ is velocity, and $s_0(\mathbf{x})$ is the initial condition at $t = t_0$. If $\mathbf{v}$ is known, then (3.1) is a linear differential equation for s.

A formal solution to (3.1) can be found through a Green's function approach (Hall and Plumb, 1994; Holzer, 1999; Holzer and Boer, 2000; Bowman and Carrie, 2002). The Green's function G is the solution to (3.1) for all possible δ-function initial conditions (all $\mathbf{x_0}$), that is,

$$\frac{\partial G}{\partial t} + \mathbf{v} \cdot \nabla G = 0, \qquad G(\mathbf{x}, \mathbf{x_0}, t_0) = \delta(\mathbf{x} - \mathbf{x_0}). \tag{3.2}$$

The principal advantage of this solution technique is that, if G can be found, the solution to (3.1) for an arbitrary initial condition $s_0(\mathbf{x})$ is given by

$$s(\mathbf{x}, t) = \int_{\mathbf{x_0}} s_0(\mathbf{x_0})\, G(\mathbf{x}, \mathbf{x_0}, t)\, d\mathbf{x_0}. \tag{3.3}$$

This approach can be easily extended to find the climatological transport properties of the atmosphere. Given an ensemble of $\mathbf{v}$ fields, (3.1) can be solved repeatedly for the same initial condition. The ensemble-mean solution $\langle s \rangle$ is found by taking the ensemble mean

of (3.3), which yields

$$\langle s(\mathbf{x},t)\rangle = \int_{\mathbf{x_0}} s_0(\mathbf{x_0})\ \langle G(\mathbf{x},\mathbf{x_0},t)\rangle\ d\mathbf{x_0}, \tag{3.4}$$

because s_0 does not vary across the ensemble. Therefore, for a specified initial distribution the ensemble-mean tracer distribution at future times can be found from the ensemble-mean Green's function. More importantly, perhaps, $\langle G\rangle$ provides a quantitative description of the climatological transport of a conserved passive tracer from an arbitrary initial location $\mathbf{x_0}$. $\langle G\rangle$ is thus one way to represent the climatological transport circulation of the atmosphere.

The function $\langle G\rangle$ could be estimated by solving the Eulerian equation (3.2) repeatedly for different $\mathbf{x_0}$ and $\mathbf{v}$, but the computational costs are high. It is possible, however, to estimate $\langle G\rangle$ from air parcel (particle) trajectories because of the close connection between the solutions to the trajectory equation

$$\frac{d\mathbf{x}'}{dt} = \mathbf{v}(\mathbf{x}',t), \qquad \mathbf{x}'(t_0) = \mathbf{x}'_\mathbf{0} \tag{3.5}$$

and the solutions to (3.2). In (3.5), $\mathbf{x}'$ is the position of the particle as a function of time t, $\mathbf{v}$ is the velocity, and $\mathbf{x}'_\mathbf{0}$ is the initial location of the particle at $t = t_0$. (Primes are used to explicitly denote a particle trajectory.)

The Green's function for (3.1) is

$$G(\mathbf{x},\mathbf{x_0},t) = \delta(\mathbf{x} - \mathbf{x}'(\mathbf{x}'_\mathbf{0},t)). \tag{3.6}$$

where $\mathbf{x}'(\mathbf{x}'_\mathbf{0},t)$ is the solution to the trajectory equation (3.5) and $\mathbf{x_0} = \mathbf{x}'_\mathbf{0}$. This occurs because the trajectories are simply the characteristics of 3.1. An alternative way of stating this result is that the transport operator simply advects the δ-function initial condition without changing its shape (in the absence of diffusion). The path followed by the δ-function is

the same as the path followed by a particle with the same initial location, $\mathbf{x_0}$. Particle trajectories can be used, therefore, to construct the Green's function. Bowman (Bowman and Carrie, 2002) discusses additional details, including sampling issues arising from particle counting.

Both forward and backward trajectories can be computed so that it is possible to evaluate both where air goes to and where it comes from.

B. Application to Texas

1. Gridded trajectories for regional-scale flow analysis

Trajectories for a rectangular region containing the state of Texas are computed using a standard 4th-order Runge-Kutta scheme with a 45 minute time step (Bowman and Carrie, 2002). Winds are interpolated to the particle locations linearly in both space and time. It is not possible to evaluate $\langle G(\mathbf{x}, \mathbf{x_0}, t) \rangle$ for all possible x_0. Instead, we evaluate $\langle G \rangle$ for a moderately-dense, discrete, three-dimensional grid of initial conditions. The initial horizontal locations are shown in Figure 2. Parcels are initialized on a regular latitude-longitude grid with horizontal spacing of ~ 30 km $\times \sim 30$ km and 18 unevenly spaced pressure levels from 998–200 hPa, giving 17,640 parcels total. Trajectories are initialized each day at 18Z at the grid locations and run 7 days forward and backward for every day in July from 1979–2000. During the summer months 18Z corresponds to 13:00 Central Daylight Time. The result is a set of 682 (22×31) forward trajectories and 682 backward trajectories for each point shown in Figure 2. These will be referred to as grid trajectories. The computation time required to run the trajectories is modest (roughly 40 hours on a single 2.8 GHz Xeon processor) .

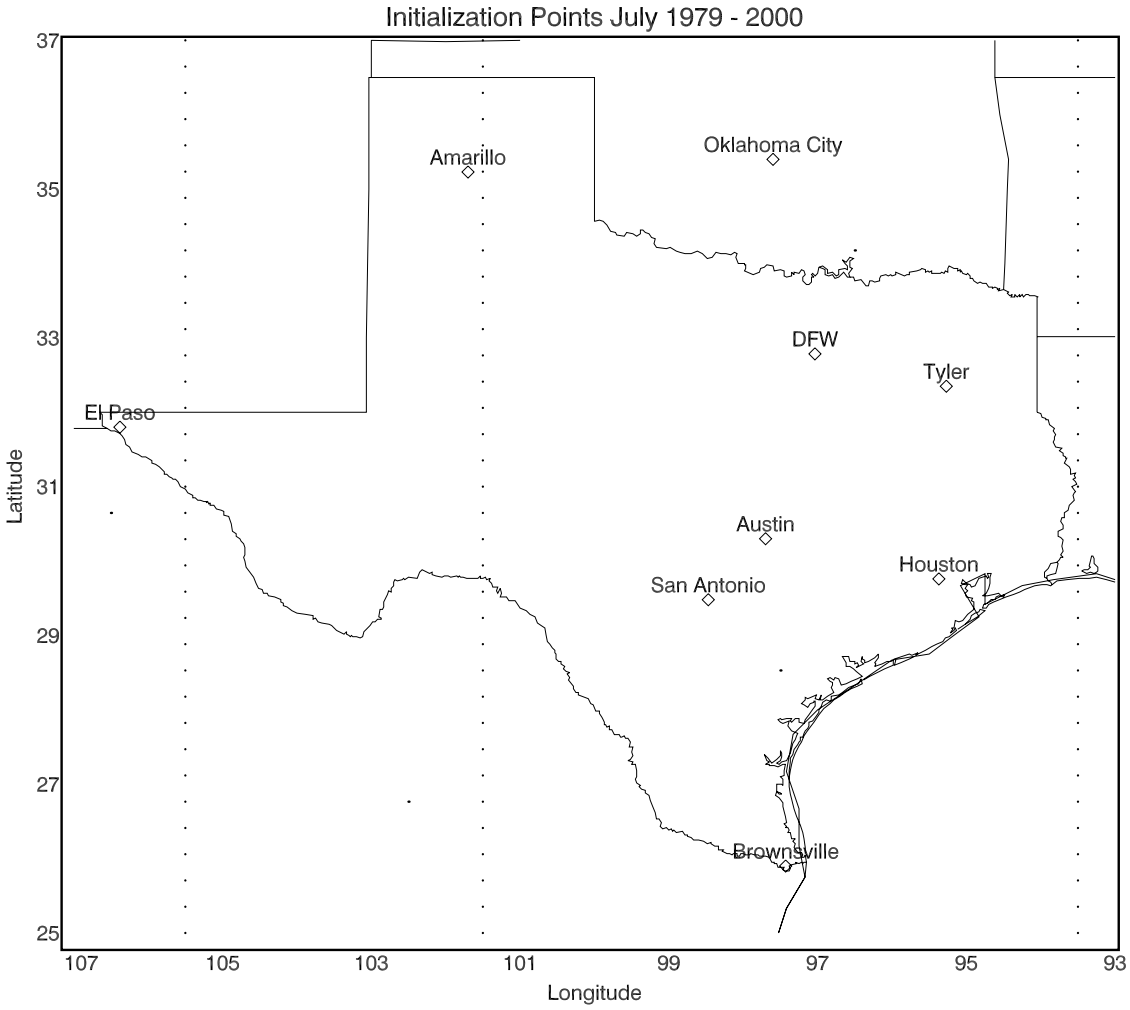

Fig. 2. Initialization points for grid trajectories.

The ensemble-mean Green's function $\langle G(\mathbf{x}, \mathbf{x_0}, t)\rangle$ is estimated by computing the discrete probability distribution function of the particles as a function of $\mathbf{x}$ for each $\mathbf{x_0}$ on the grid at desired times. The destination grid $\mathbf{x}$ does not have to match the initial location grid $\mathbf{x_0}$. For later illustrations, subsets of $\langle G\rangle$ are made of the grid trajectories for four urban areas: Austin, Dallas/Fort Worth, Houston, and San Antonio. The subsets are composed of all the grid trajectories initialized at points surrounding each urban area (Figure 1). The geographically larger areas of Dallas/Fort Worth and Houston are composed of four grid points, while Austin is composed of two, and San Antonio of one. The distributions are for illustration purposes only and do not represent the actual distribution of sources in these metropolitan areas. Air particle locations in the urban trajectories are plotted every six hours, and contours are drawn showing the density of particles as they disperse (climatologically) from the initial location, normalized by the maximum density. These correspond to slices through the multidimensional Green's function. Only particles initialized at the lowest 7 altitudes, less than approximately 850 hPa, are plotted. Particles above 850 hPa typically lie above the boundary layer and are not influenced by surface sources on short timescales. In this way a probability distribution of low-level particle transport is created for particles released from the four urban areas at 18Z in July.

2. Statistical analysis of back trajectories

Additional backward trajectories are computed using the 5 selected CAMS ozone monitoring sites as initialization points. In detail, the 5 selected CAMS stations are Aldine C8, Cypress River C50, Fort Worth Northwest C13, Longview C19, and Tyler Airport C86. Additional trajectories are run for 95 other CAMS stations, but are not studied due to their location, quality of data, or length of data collection. In all other ways the trajectories are the same as the previously discussed grid trajectories, except they are initialized at each hour (00Z–23Z) and run 2 days backward for every day in July, August, and September

from 1979–2000. The result is a set of 48,576 backward trajectories from each of the 5 CAMS stations. The computation time to run the trajectories is roughly 180 hours on a single 2.8 GHz Xeon processor.

The backward station trajectories are assigned the ozone values recorded at the time of their initialization at the CAMS stations where they are initialized. Only months during which an ozone exceedance was recorded are discussed. First, the two-day backward trajectories initialized at Longview C19 from 1996-1999 are grouped by month, either July, August, or September, and divided into groups based on ozone value. Trajectories from Tyler Airport C86 for August, the only month during which exceedances were recorded, of 1996-1999 are also subdivided. Trajectories from Aldine C8 and Fort Worth Northwest C13 are studied when an exceedance at either coincides with an exceedance at Longview C19 or Tyler Airport C86. Rural ozone exceedances at Longview C19 and Tyler C86 are of primary interest in this study, so urban exceedances are studied only when they coincide with rural exceedances as a way of relating air quality around the state. Trajectories from the station Cypress River C50 for July 1997-2000 rather than 1996-1999 are used since the only ozone exceedances ever recorded at this station occurred in July of 2000. Although Cypress River C50 only recorded ozone exceedances on one day during July from 1997-2000, trajectories from the station are used in the study due to its proximity to Longview and Tyler and the rural nature of its surroundings.

The trajectories are divided into four groups based on the ozone value at the station at each trajectory's initialization time. Ozone values of 0-40 ppm are considered low, 41-80 ppm moderate, 81-124 ppm high, and 125 ppm or greater are exceedances. Changes in the cutoff values of each group by up to 15 ppm did not result in significant changes in the statistical characteristics of the trajectories. The statistical characteristics of each group are

then investigated.

3. Exceedance case studies

Synoptic conditions for the three-day period surrounding exceedances are determined from plots of geopotential height made using NCEP Reanalysis data. Additionally, surface meteorological plots created by Unisys Weather are studied to evaluate the synoptic situation. The 48-hour backward trajectories computed from the 5 selected CAMS stations at the time of each exceedance using NCEP Reanalysis winds are studied as well. The synoptic plots, backward station trajectories, and ozone values are compared to determine what conditions are prevalent when ozone exceedances occur. Similarly to the CAMS Lagrangian trajectories, ozone exceedances at the 5 CAMS sites occurring in the summer months from 1996-1999 or 1997-2000 are studied. In all thirty-five one-hour ozone exceedances, meaning one-hour ozone values greater than or equal to 125 ppm will be discussed. Details of the ozone exceedances occurring at these five stations in the summer months from 1996–2000 are shown in Table II and will be referred to by an event number from this point on.

Longview and Tyler are small cities with a population of less than 85, 000 each. Jefferson, which is near the station Cypress River C50, is a small town with a population of 2200. The three cities are all within 100 km of each other, and are approximately 200 km east of Dallas/Fort Worth and 250 km north of Houston. A histogram of the daily maximum one-hourly ozone values from 1997–2000 at Cypress River C50 in July, as well as Longview C19 and Tyler Airport C86 from 1996–1999 in August is shown in Figure 3. Cypress River C50 has the most daily maximum one-hourly values of the three stations in the range termed ”healthy” by the TCEQ, or values between 0 and 79 ppm. The number of ”healthy” values at Cypress River C50 is likely due in part to the comparatively small population of Jefferson. Of the daily maximum one-hourly ozone values at Cypress River C50 73%

are healthy, compared to 49% of those at Longview C19 and 33% at Tyler Airport C86. Longview C19 with 51%, and Tyler Airport C86 with 58%, recorded similar percentages of values between 80 and 124 ppm, considered ”moderate” by the TCEQ. In comparison only 26% of ozone values recorded at Cypress River C50 are considered moderate. Finally, only one day in the period of study resulted in ”unhealthy for sensitive groups” ozone values at Cypress River C50 and Tyler Airport C86, while four days had values of greater than or equal to 125 ppm at Longview C19. The other two stations studied, Aldine C8 and Fort Worth Northwest C13, are located approximately 10 km southwest of downtown Houston and 10 km northwest of downtown Fort Worth, respectively.

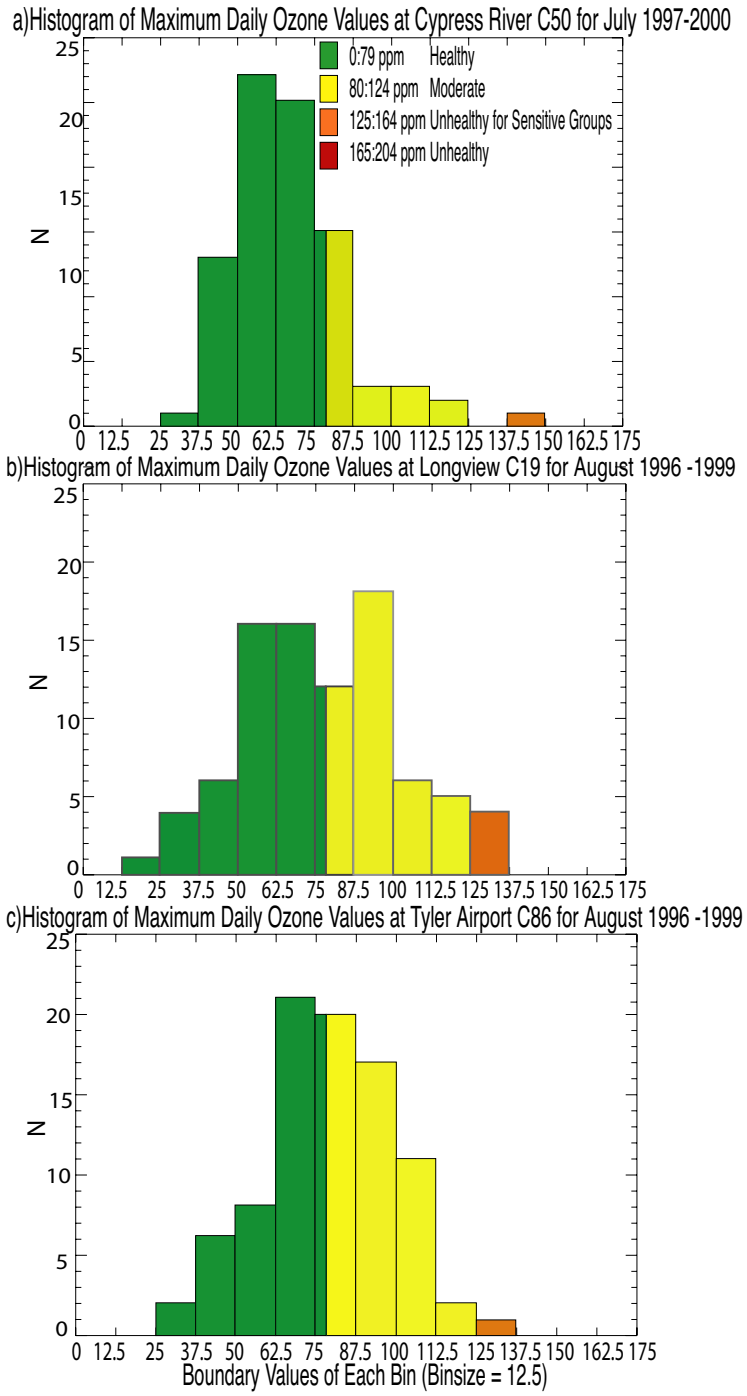

Fig. 3. Histogram of daily maximum one-hourly ozone values at a) Cypress River C50 during July 1997–2000, b) Longview C19 during August 1996–1999, and c) Tyler Airport C86 during August 1996–1999.

Table II. A summary of ozone exceedances recorded at 5 selected CAMS stations in July, August, and September from 1996–2000.

Event	Station	Latitude Longitude	Date	Time (GMT)	Length (Hrs)	Peak Ozone (ppm)	Summary
1	Longview C19	32.382N 94.712W	1997-07-16	16	1	139	Front passes 36 hrs before exceedance
2	Longview C19	32.382N 94.712W	1998-08-16	19	1	127	Stagnant trajectory from high pressure aloft
3	Longview C19	32.382N 94.712W	1998-08-28	19	1	129	Front passes 4 hours after exceedance
4	Longview C19	32.382N 94.712W	1998-09-03	22	1	125	Trough passes 6 hours before exceedance
5	Aldine C08	29.901N 95.326W	1998-09-03	17-20	4	143	Trough passes at 17 GMT
6	Aldine C08	29.901N 95.326W	1998-09-04	2,3,12-14	5	155	High pressure after trough stalls
7	Fort Worth NW C13	32.806N 97.357W	1999-08-03	20	1	132	Front passes 8 hours before exceedance
8	Fort Worth NW C13	32.806N 97.357W	1999-08-04	18-21	4	164	Cold front stalls to south and moves north
9	Fort Worth NW C13	32.806N 97.357W	1999-08-05	18-21	4	154	High pressure devel-ops at 12 GMT
10	Longview C19	32.382N 94.712W	1999-08-04	16	1	132	Cold front stalls to south and moves north
11	Tyler Airport C86	32.358N 95.410W	1999-08-05	17-21	5	127	High pressure devel-ops at 12 GMT
12	Longview C19	32.382 94.712NW	1999-08-17	21-23	3	134	High pressure moves in 30 hours after front
13	Longview C19	32.382 94.712NW	1999-09-20	16	1	138	Trough passes 3 hours after exceedance
14	Cypress River C50	32.743N 94.303W	2000-07-16	20-22	3	149	High pressure, strong dryline to west

CHAPTER IV

RESULTS

A. Results from Green's function method

1. Climatological Eulerian flow field

Figure 4 shows the climatological geopotential height at 850 hPa over Texas during July. Lower heights over west Texas indicate the semi-permanent area of low pressure in the desert southwest known as the North American thermal low (NATL). West Texas experiences the eastern portion of the counter-clockwise circulation around this low. Higher heights in east Texas are connected to the semi-permanent area of high pressure in the Caribbean and eastern Atlantic known as the Bermuda High. Central and east Texas are influenced by the western edge of the clockwise circulation around this area of high pressure. Texas lies within the transition zone between these two pressure areas and typically experiences widespread southerly flow during the summer months. The geopotential height climatology allows us to anticipate that the general character of the particle trajectories in the lower atmosphere will be northward.

2. Probability distribution of Houston air particles

As an example, the climatological transport from the Houston area is shown in Figure 5 at 6, 12, and 24 hours after the particle release time. The four corners of the black rectangle surrounding Houston represent the initial points of the Houston urban subset; dots represent the individual air particles initialized at altitudes below 850 hPa; and the contours represent the probability density normalized by the peak density value (peak = 1). The distributions show that the clockwise circulation around the Bermuda High dominates the transport of particles during July. Particles move north and then east. Figure 5a shows

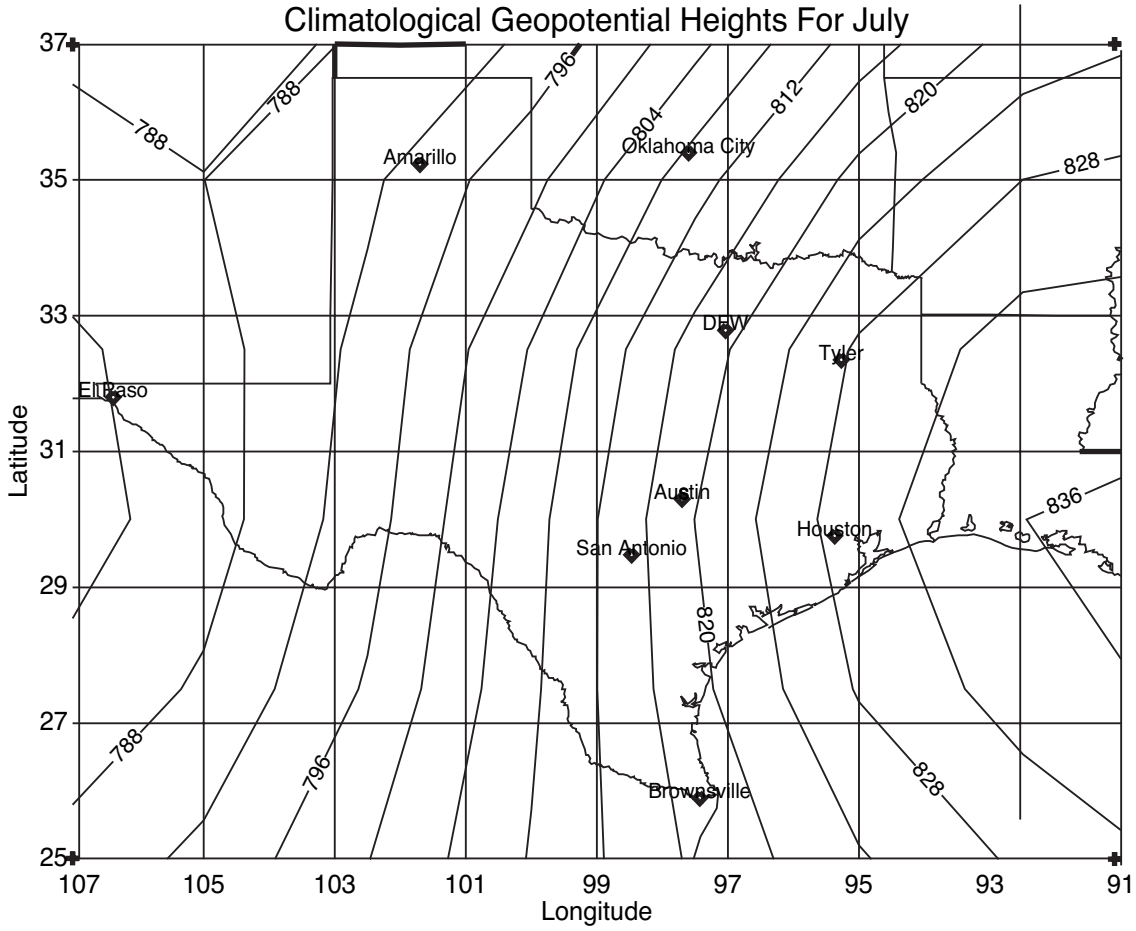

Fig. 4. Climatological geopotential height at 850 hPa for July (in meters).

that 6 hours after release the probability distribution of the particles is essentially circular. The particles move north and are most likely to be approximately 110 km north-northeast of downtown Houston (mean speed of 5.4 $m \cdot s^{-1}$). Figure 5b shows that 12 hours after release the distribution remains nearly circular. The particles have continued moving north and are now centered about 240 km north of downtown Houston over rural east Texas (mean speed of 5.5 $m \cdot s^{-1}$). Tyler, a town of 83,650 with occasional summer ozone exceedances attributed to air transported from Houston (Texas Commission on Environmental Quality in Austin, Texas, 2000), lies within the 0.6 isopleth at 12 hours . Figure 5c shows that 24 hours after initialization the probability distribution is still roughly circular. Particles have moved far enough north to enter the northern edge of the clockwise circulation and have begun to move east (mean speed of 7.1 m/s). The distribution is centered over Texarkana, roughly 600 km from downtown Houston. The increase in mean speed with increasing time is due to some of the particles moving to higher altitudes where mean wind speeds are larger.

3. Vertical distribution of Houston air particles

The vertical distribution of particles 6, 12, and 24 hours after their release in Houston is shown in Figure 6. The obvious layering evident in Figure 6a is a result of the initialization of particles at 7 discrete levels below 850 hPa. Figure 6b shows that the rate of northward particle motion increases with altitude. A small fraction of the particles move southward. Similarly, continued northward motion which is much greater above 900 hPa is evident in Figure 6c . The increase in the northward movement of the particles with altitude is evidence of increasing wind speed aloft.

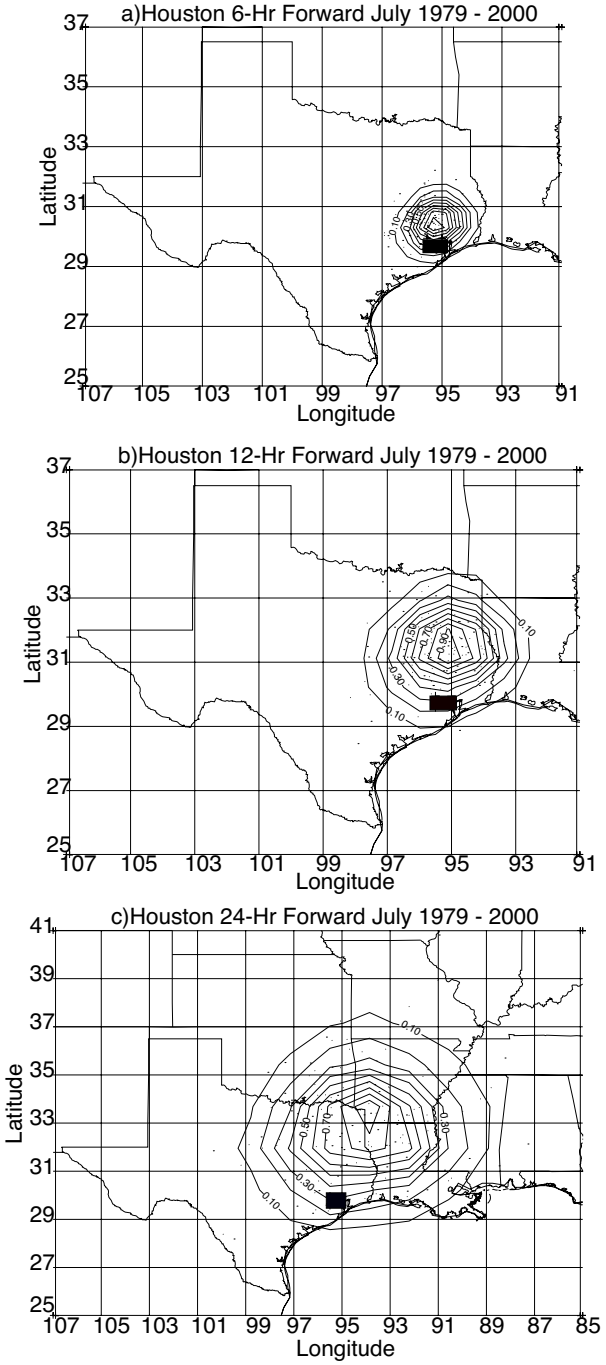

Fig. 5. Probability distributions for the Houston urban subset (a) 6, (b) 12, and (c) 24 hours after initialization at 18Z.

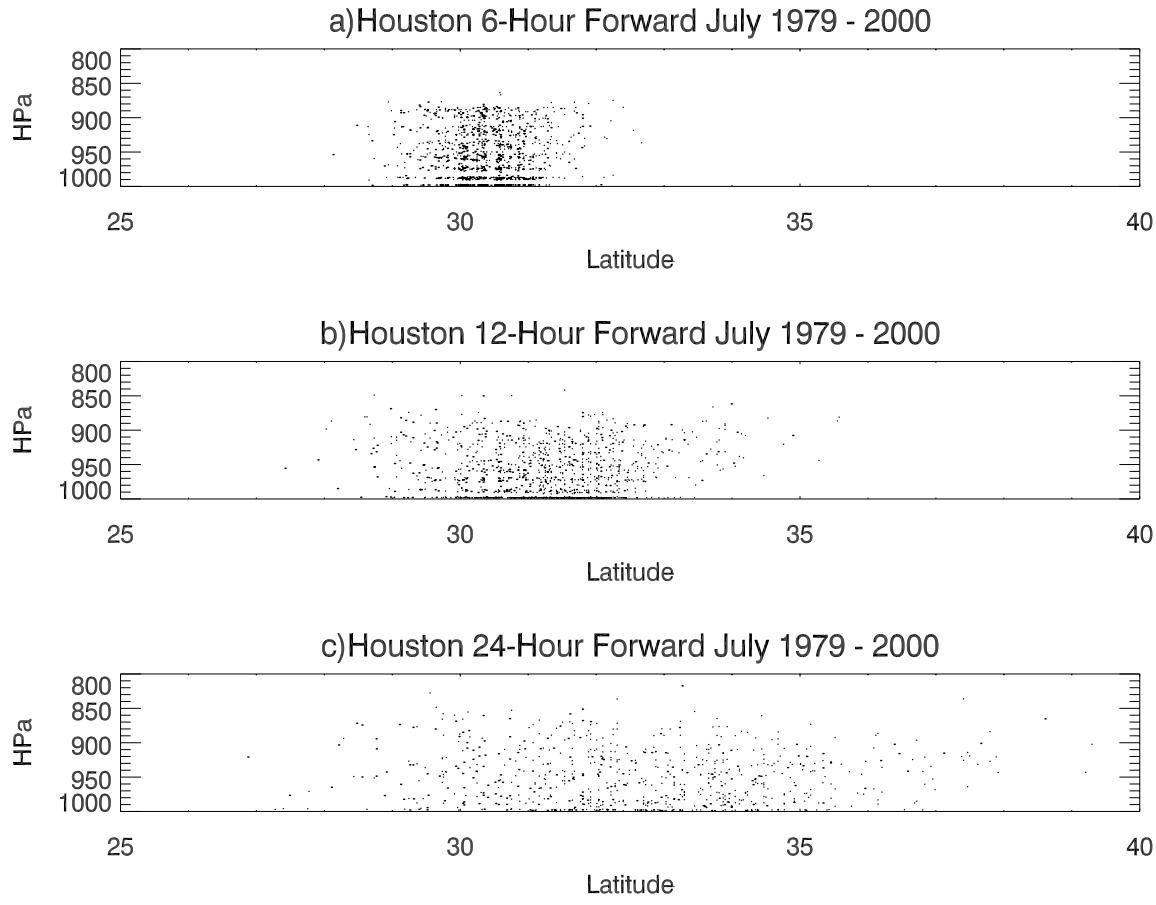

Fig. 6. Vertical distributions for the Houston urban subset (a) 6, (b) 12, and (c) 24 hours after initialization at 18Z.

4. Applications of Green's functions

As discussed previously, if the value of $\mathbf{x_0}$ is fixed, $\langle G(\mathbf{x}, \mathbf{x_0}, t)\rangle$ describes how air initially at $\mathbf{x_0}$ disperses throughout the atmosphere as a function of t in a climatological

sense. $\langle G \rangle$ can be used to calculate an approximate solution for the evolution of an arbitrary initial distribution, including, for example, both widespread (e.g., biogenic) sources and urban-scale sources, by summing appropriately weighted sources at various initial locations. Figures 7a–7c show $s(\mathbf{x}, t)$ at 6, 12, and 24 hours for an initial condition that is a combination of localized sources around all four metropolitan areas listed above. For illustration purposes, the initial condition for each urban area is a value of 1, while the remaining initial conditions at all other latitudes and longitudes are assigned a value of 0. The value of s is then calculated using (3.3). The resulting plots show the climatological probability density of the combined transport from the four urban centers as a function of t. By adding appropriately-weighted solutions for multiple initial times it is also possible to simulate plumes from steady or time-varying sources (not shown).

Similarly, Figures 8a–8c show $s(\mathbf{x}, t)$ at 6, 12, and 18 hours backwards in time for a final condition of 1 at Dallas. The resulting plots show the climatological probability density of sources of air transported toward Dallas as a function of t. To elaborate, Figure 8a is a plot of the climatological probability density of transport 6, 12, and 24 hours prior to arriving at the initial condition of 1 assigned to the latitude and longitude corresponding to Dallas. It can be observed that Austin and San Antonio lie within the plotted climatological probability density in Figure 8c, while Houston lies on its eastern edge. Climatologically (and within the resolution of the NCEP data) air in Dallas is unlikely to have passed through Houston in the previous 18 hours.

If the climatological ensemble-mean Green's function $\langle G(\mathbf{x}, \mathbf{x_0}, t) \rangle$ is known, then the ensemble-mean trace substance distribution $\langle s(\mathbf{x}, t) \rangle$ can be computed at any location and time by using (3.4). From $\langle s(\mathbf{x}, t) \rangle$ a variety of derivative quantities can be found. These

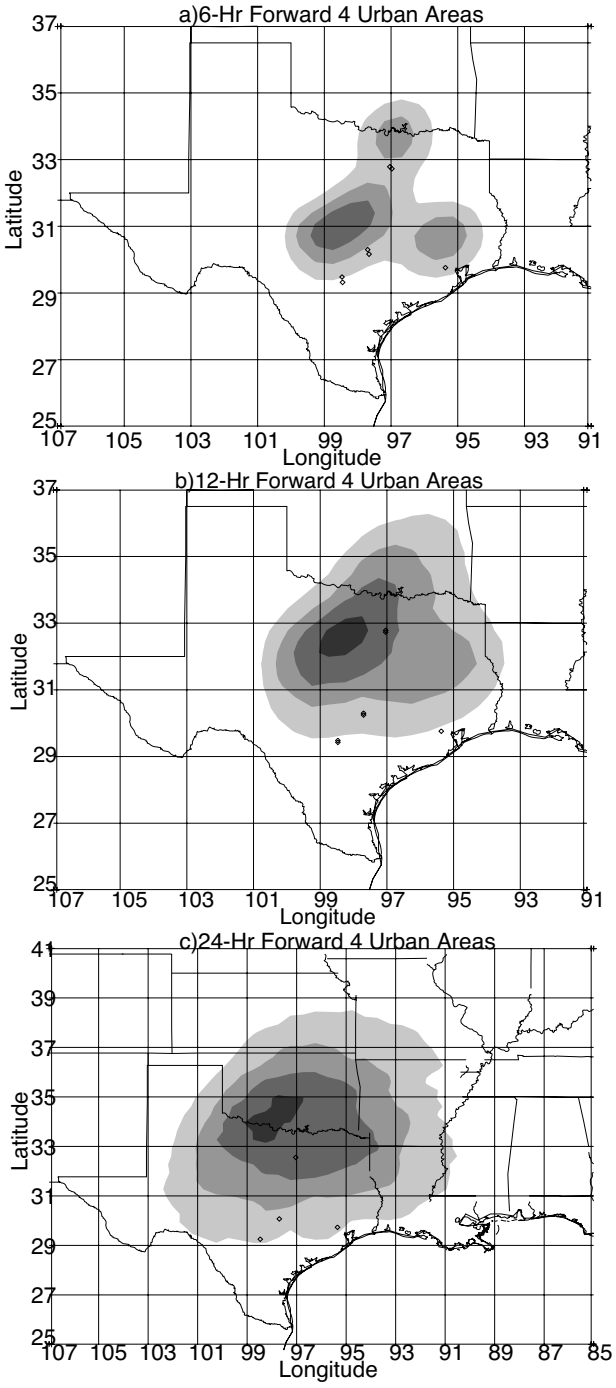

Fig. 7. $S(\mathbf{x}, t)$ with $\mathbf{x_0}$ of 1 at Houston, San Antonio, Dallas, and Austin and t of 6, 12, and 24 hours.

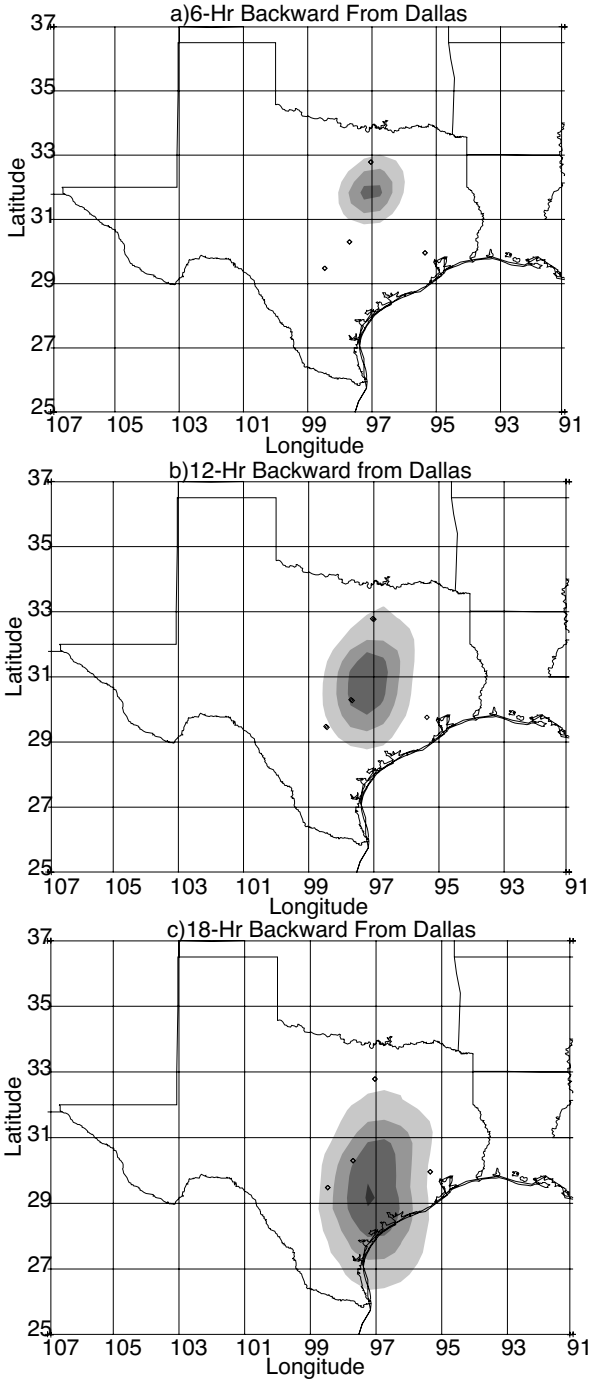

Fig. 8. $S(\mathbf{x}, t)$ with $\mathbf{x_0}$ of 1 at Dallas and t of 6, 12, and 24 hours.

include the area-mean concentration of $\langle s \rangle$ over a destination region $\mathbf{x_D}$

$$s_D(t) = \frac{\int_{\mathbf{x_D}} s(\mathbf{x}, t)\, d\mathbf{x}}{\int_{\mathbf{x_D}} d\mathbf{x}}, \tag{4.1}$$

and the fractional amount of $\langle s \rangle$ within the region $\mathbf{x_D}$ at time t

$$f_D(t) = \frac{\int_{\mathbf{x_D}} s(\mathbf{x}, t)\, d\mathbf{x}}{\int_{\mathbf{x}} s_0(\mathbf{x}, t_0)\, d\mathbf{x}}. \tag{4.2}$$

The quantity f_D is directly related to the climatological probability that an air parcel from an initial distribution of parcels will fall within the region $\mathbf{x_D}$ at time t (Hall and Plumb, 1994).

Plots of $f_D(t)$ illustrate how the average concentration of a trace substance at destination changes with respect to t for an ensemble of identical sources. Figure 9 shows sample results for two sources, Houston and San Antonio, and two destinations, Tyler and Dallas. The destinations are the latitudes and longitudes of Tyler and Dallas. Figure 9 shows $f_D(t)$ for three cases: Houston to Tyler, Houston to Dallas, and San Antonio to Dallas. In each case the probability rises from zero, reaches a maximum, and then decreases more slowly. The peak in the curve occurs later when the transport distance is larger. The maximum value of f_D at 18 hours in the Houston to Dallas case is only .0045, compared to a maximum for f_D of .0125 in the Houston to Tyler case, showing that Tyler is more than 2.5 times more likely to be influenced by air from Houston than is Dallas. In comparison, transport from San Antonio to Dallas begins to increase 6 hours after initialization, peaks with a value of .0025 at 24 hours and then begins a gradual decrease. Dallas is consistently influenced more by air from Houston than by air from San Antonio over the 48 hour period shown.

Figure 9 is a plot of the absolute values of f_D for different strength sources. The solid line represents transport from Houston to Tyler, the asterisk line represents transport from

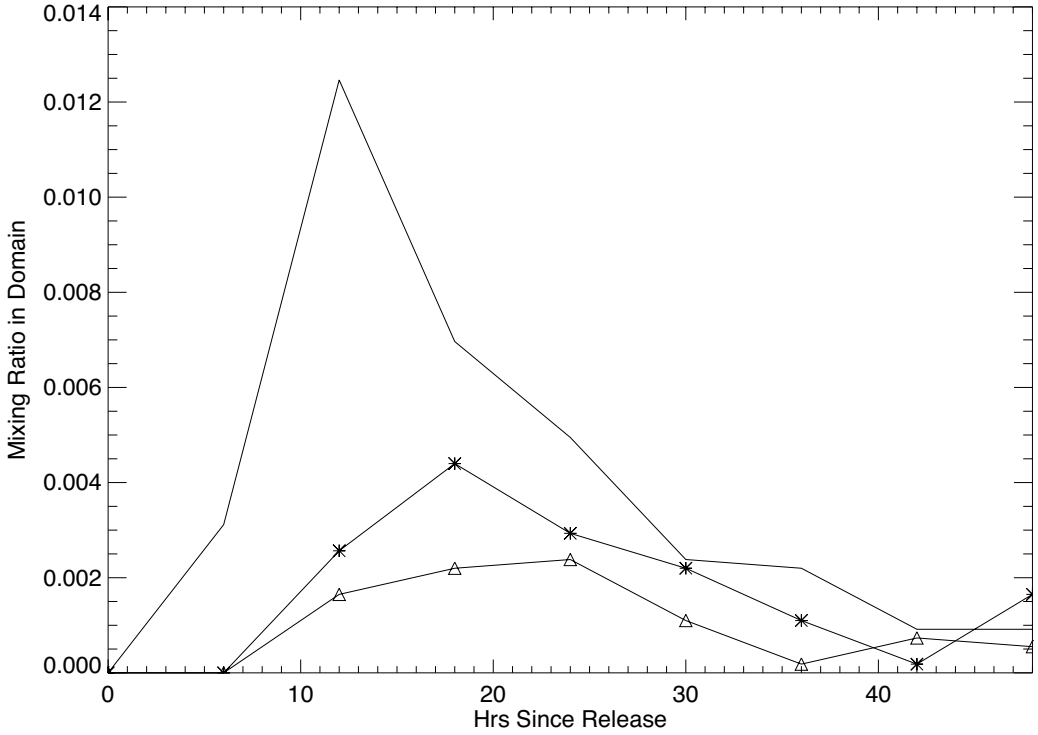

Fig. 9. Probability that an air parcel from the source region will lie within the destination region as a function of time from release.

Houston to Dallas, and the triangle line represents transport from San Antonio to Dallas. The value of f_D for transport from Houston to Dallas is greater than the value of f_D for transport from San Antonio to Dallas since four grid points were used to initialize grid trajectories in Houston compared to one grid point in San Antonio. The grid trajectories were then used to calculate $\langle G \rangle$. In contrast, Figure 8 is a plot of the climatological probability density of particles normalized by the total number of particles. Thus, while the density of particles transported to Dallas from San Antonio is greater than the density of particles transported to Dallas from Houston, the numeric value of $\langle G \rangle$, and as a result f_D, is greater from Houston to Dallas due to the larger number of particles. In this manner $\langle G(\mathbf{x}, \mathbf{x_0}, t) \rangle$ can be applied to compare the relative likelihood that transport from different sources will affect a chosen destination.

B. Statistical analysis of back trajectories from CAMS sites

In this section the statistical characteristics of ozone levels and backward trajectory paths from the five selected CAMS stations are investigated. The period of study is the summertime months from 1996–1999, except for the case of Cypress River C50, for which the years 1997–2000 are used. For each month (all years) the trajectories are divided into four groups based on the ozone value at the station at the time each trajectory arrives at the station. Ozone values of 0–40 ppm are considered low, 41–80 ppm moderate, 81–124 ppm high, and 125 ppm or greater are exceedances. The results are discussed below and are organized by CAMS site and month. One aim of this analysis is to determine whether ozone levels at these rural sites are influenced primarily by local pollution sources within Texas or by air transported from outside the state.

1. Longview C19

a. July

Figure 10 shows the back trajectories for parcels arriving at Longview C19 in July stratified by the 1-hour ozone concentration at the time of arrival. Red lines are drawn through the locations of each CAMS stations where they approximately divide the trajectories approaching from distinctly different directions. The trajectories are then qualitatively divided into parcels that pass primarily over Texas in the prevailing summertime southerly flow and those that come from the east and north. The two groups are distinguished somewhat arbitrarily by which side of the red line they lie on 24 hours before arriving at the station. The figures, however, show 48-hour backward trajectories to better illustrate directional changes of the trajectories with time. For readability, not all of the trajectories are shown in graphs that have large numbers of trajectories. For each ozone category the fraction of the particles arriving from each side of the line is given in the NE and SW corners of the maps and summarized in the table below. Table III gives the percentages of each group of trajectories arriving at Longview C19 in July from both sides of the line. The location of the CAMS station of interest is shown as a red diamond.

For this site and month, in every group except the exceedances (for which there are only two trajectories), the majority of the trajectories come from the left side. Overall, only 21% of the total trajectories come from the right side. However, 33% of the high level and 100% of the exceedance level trajectories come from the right side. This indicates that high ozone levels are more likely to be associated with transport from the north and east than low and moderate ozone values at Longview in June.

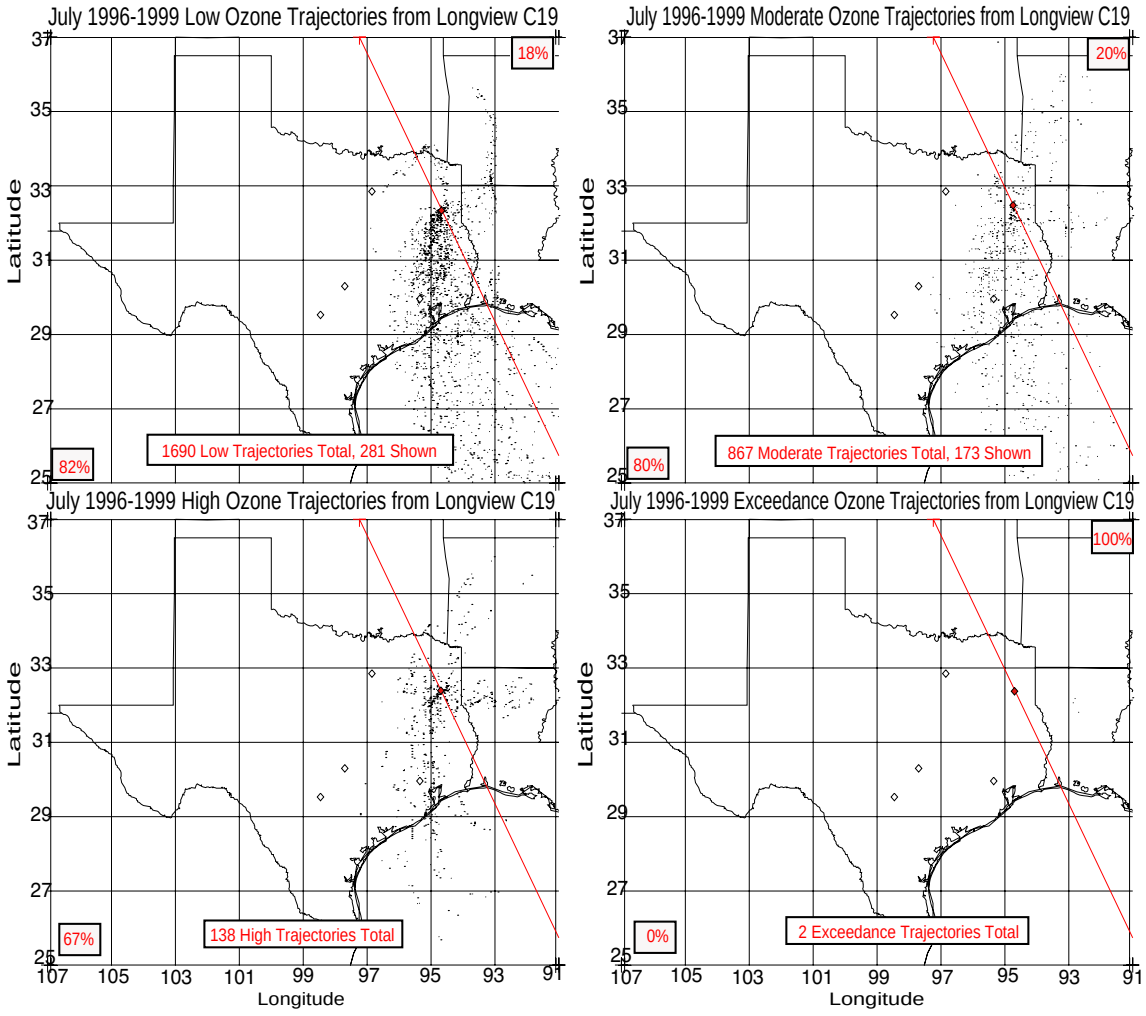

Fig. 10. Forty-eight-hour back trajectories for low, moderate, high, and exceedance ozone measurements at Longview C19 during July 1996–1999.

Table III. Percentages of low, moderate, high, and exceedance ozone trajectories that come from each side of the red line in Figure 10 for Longview C19 during July 1996–1999.

Site: Longview C19, July

Category	Left side	Right side	Number
Low	82%	18%	1690
Moderate	80%	20%	867
High	67%	33%	138
Exceedance	0%	100%	2
Total	79%	21%	2697

b. August

In August the situation is very similar as apparent from Figure 11 and Table IV. In general, while the majority of all the trajectories come from the left, the majority come from the right for the three higher ozone-level categories. This indicates an even stronger relationship in August than in July between transport from the north and east and higher level ozone values.

c. September

As seen in Figure 12 and Table V, a similar majority of the trajectories approach from the right for all four groups during September. This is likely due to the change from the summertime southerly flow off the Gulf, to more northerly flow resulting from an increase

Table IV. Percentages of low, moderate, high, and exceedance ozone trajectories that come from each side of the red line in Figure 11 for Longview C19 during August 1996–1999.

Site: Longview C19, August

Category	Left side	Right side	Number
Low	64%	36%	1594
Moderate	48%	52%	949
High	45%	55%	225
Exceedance	34%	66%	6
Total	57%	43%	2774

Table V. Percentages of low, moderate, high, and exceedance ozone trajectories that come from each side of the red line in Figure 12 for Longview C19 during September 1996–1999.

Site: Longview C19, September

Category	Left side	Right side	Number
Low	29%	71%	1623
Moderate	27%	73%	974
High	33%	67%	138
Exceedance	0%	100%	2
Total	28%	72%	2737

in frontal passages.

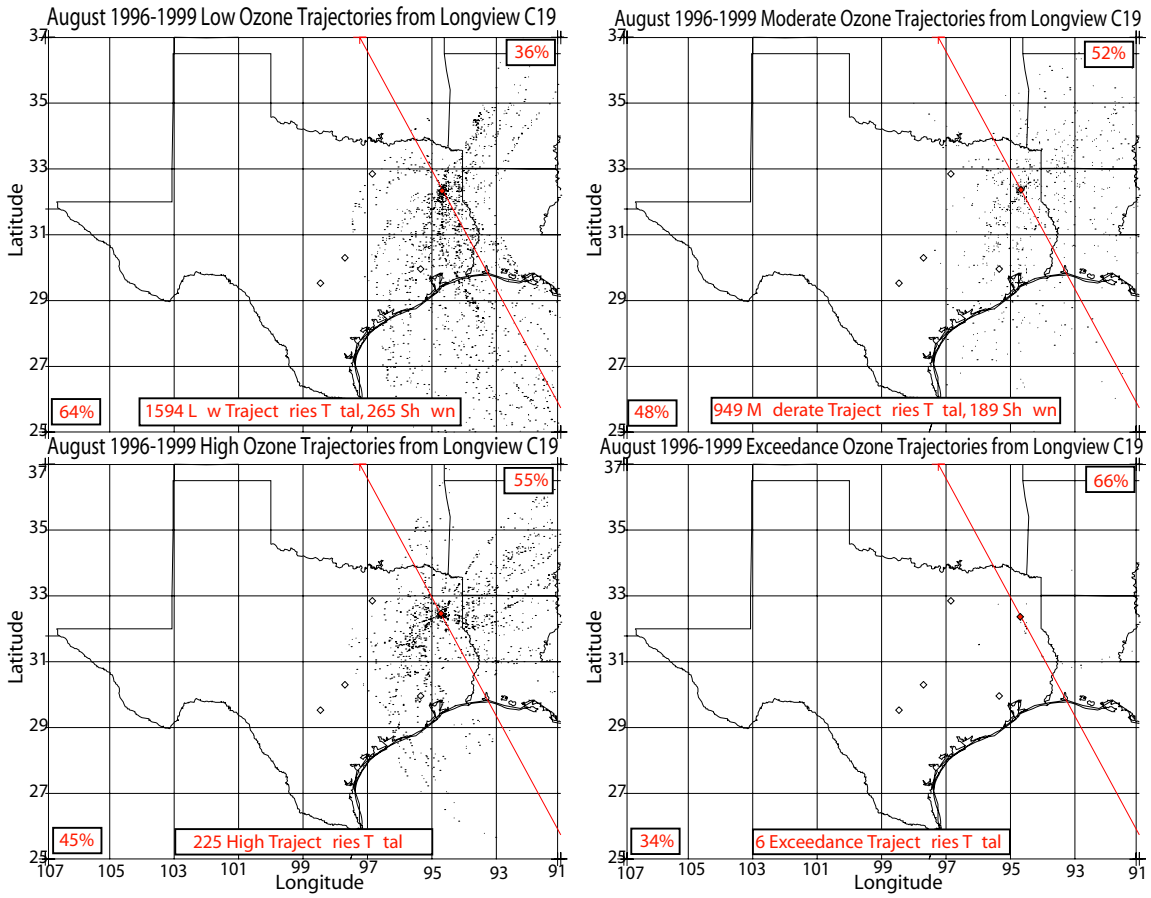

Fig. 11. Forty-eight-hour back trajectories for low, moderate, high, and exceedance ozone measurements at Longview C19 during August 1996–1999.

2. Tyler Airport C86

a. August

Trajectories from Tyler Airport C86 (32.36N, -95.41W), approximately 75 km west of Longview C19, for August 1996-1999 resemble those from Longview C19 for August. While Figre 13 and Table VI make it apparent that a slight majority of all the trajectories approach from the left, the percentage of trajectories approaching from the right side of the

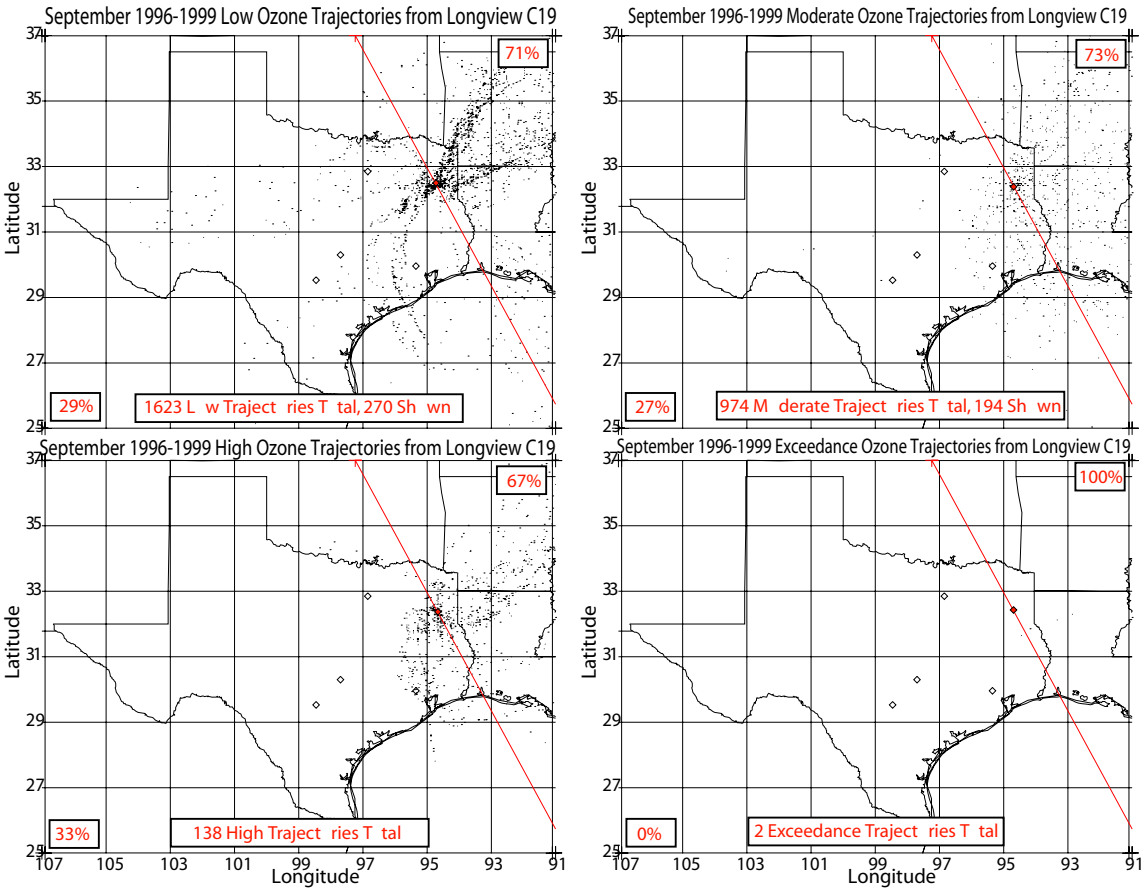

Fig. 12. Forty-eight-hour back trajectories for low, moderate, high, and exceedance ozone measurements at Longview C19 during September 1996–1999.

line increases with ozone value.

Table VI. Percentages of low, moderate, high, and exceedance ozone trajectories that come from each side of the red line in Figure 13 for Tyler C86 during August 1996–1999.

Site: Tyler C86, August

Category	Left side	Right side	Number
Low	53%	47%	1340
Moderate	54%	46%	1194
High	26%	74%	239
Exceedance	0%	100%	5
Total	51%	49%	2778

3. Cypress River C50

a. July

In contrast, the trajectories for July 1997-2000 from Cypress River C50 (32.74N, -94.30W), approximately 60 km northeast of Longview C19, do not resemble the July and August trajectories from the nearby stations of Longview C19 and Tyler Airport C86. The only ozone exceedances to occur at Cypress River C50 occurred in 2000, so the time period used was shifted from 1996-1999 to 1997-2000. In Figure 14 the majority of the trajectories from Cypress River C50 approach from the left side of the line for all four groups. In fact as Table VII illustrates, the percentage of trajectories approaching from the left side of the line remains almost constant despite changes in ozone value. However, the trajectories from Cypress River C50 may not be as dissimilar from those from nearby stations as they initially appear. All three of the exceedances shown at Cypress River C50 occurred in the same event, coming from the left side of the line, and amount to the only ozone exceedances ever recorded at the station. Furthermore, only 56 high ozone values were recorded at

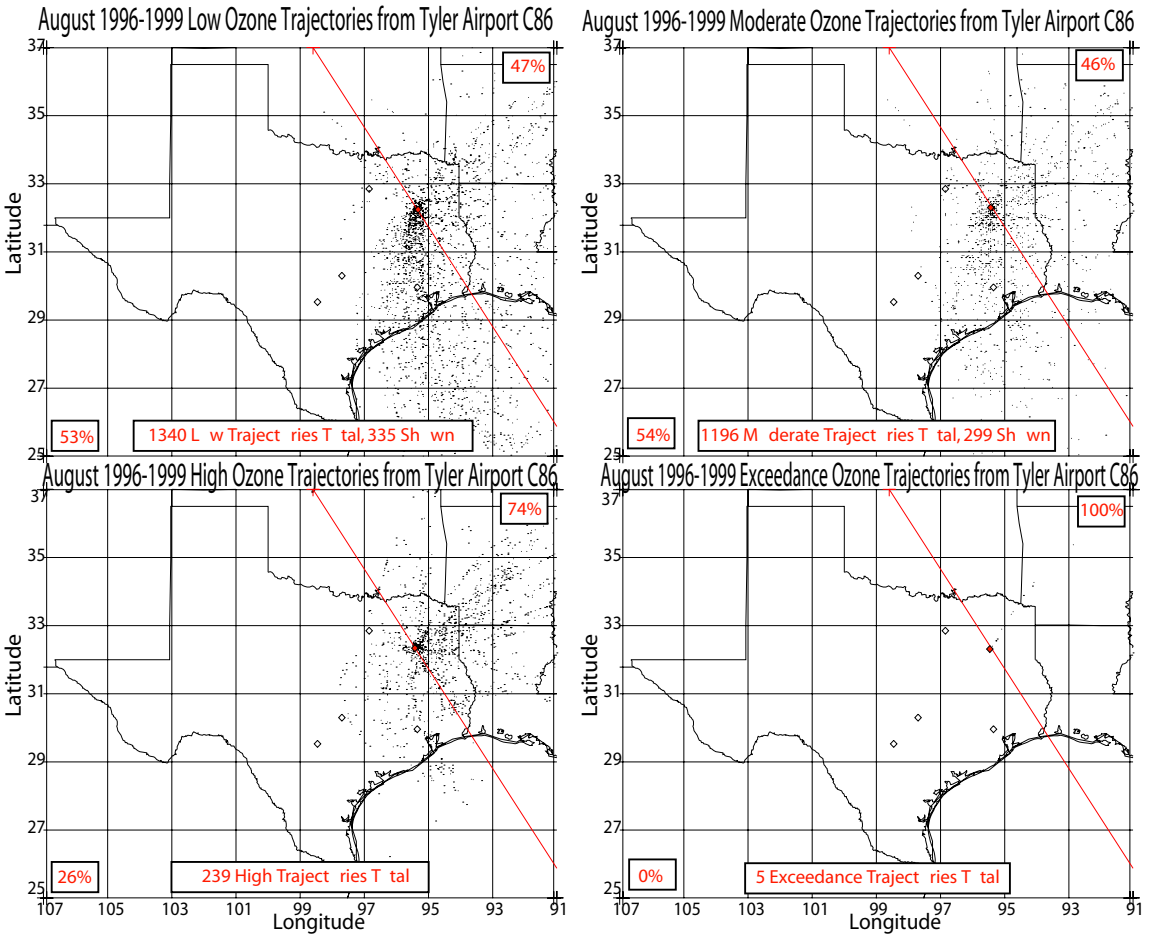

Fig. 13. Forty-eight-hour back trajectories for low, moderate, high, and exceedance ozone measurements at Tyler Airport C86 during August 1996–1999.

Cypress River C50 in July 1997-2000, compared to 106 at nearby Longview C19. The small sample size for high and exceedance-level ozone values at Cypress River C50 may not indicate the relationship between increasing ozone value and direction of approach as well as data from nearby stations.

Table VII. Percentages of low, moderate, high, and exceedance ozone trajectories that come from each side of the red line in Figure 14 for Cypress River C50 during July 1997–2000.

Site: Cypress River C50, July

Category	Left side	Right side	Number
Low	79%	21%	1340
Moderate	78%	22%	546
High	82%	18%	56
Exceedance	100%	0%	3
Total	79%	21%	1945

4. Fort Worth Northwest C13

a. August

The station Fort Worth Northwest C13 (32.81N, -97.36W) is approximately 215 km west of Tyler Airport C86. Similarly to the August trajectories from Tyler Airport C86 and the July and August trajectories from Longview C19, while the majority of all the trajectories approach from the left, the percentage of trajectories approaching the station from the right side of the line increases with ozone value. This indicates a relationship in Fort Worth in August, that can be seen in Figure 15 and Table VIII, between higher level ozone values and transport from the north and east.

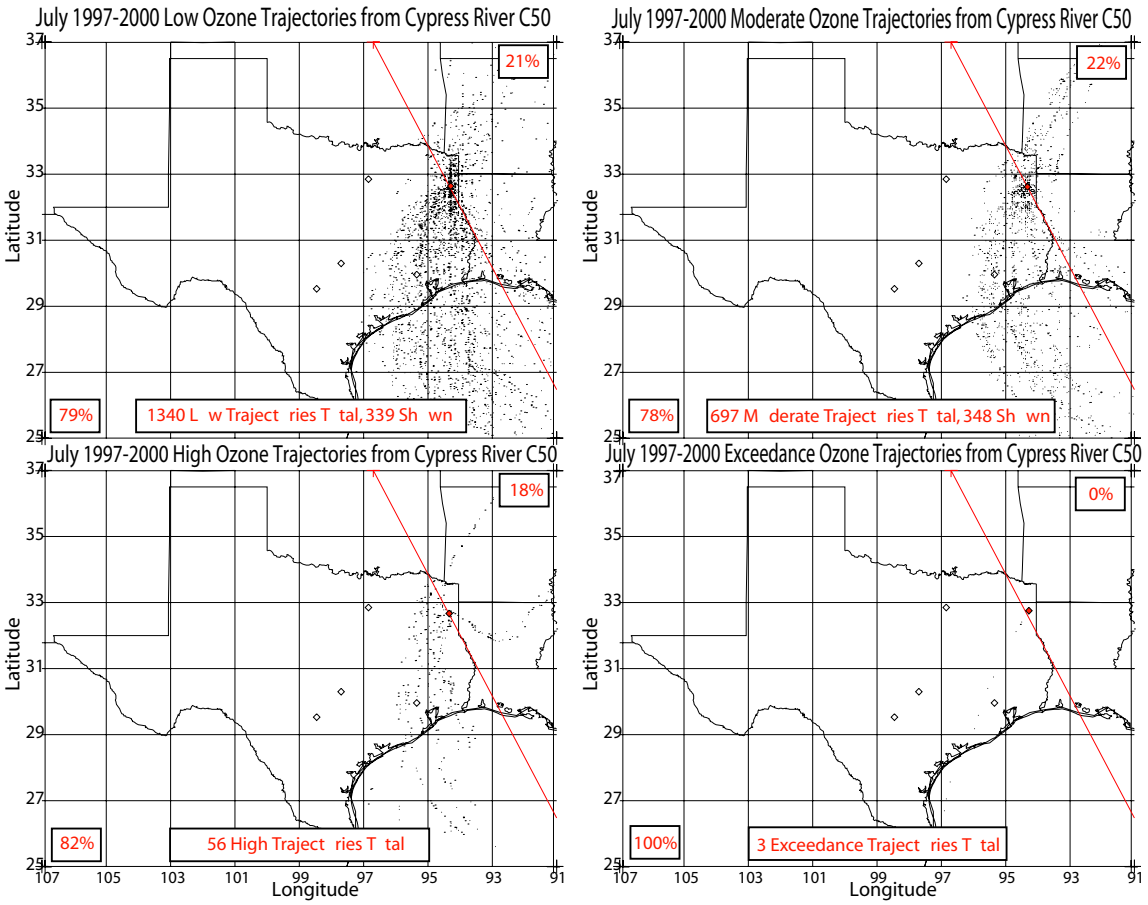

Fig. 14. Forty-eight-hour back trajectories for low, moderate, high, and exceedance ozone measurements at Cypress River C50 during July 1997–2000.

5. Aldine C8

a. September

Trajectories from Aldine C8 (29.90N, -95.33W) for September 1996-1999, shown in Figure 16 and described in Table IX, have roughly equal percentages approaching the station on the right side of the line for the low-ozone, moderate-ozone, and high-ozone trajectories, with a sharp decrease in the percentage approaching from the right for the

Table VIII. Percentages of low, moderate, high, and exceedance ozone trajectories that come from each side of the red line in Figure 15 for Fort Worth Northwest C13 during August 1996–1999.

Site: Fort Worth Northwest C13, August

Category	Left side	Right side	Number
Low	66%	34%	1781
Moderate	61%	39%	774
High	34%	66%	254
Exceedance	9%	91%	11
Total	61%	39%	2820

exceedance-ozone trajectories. The fact that the majority of trajectories approach from the right for the three lowest groups is similar to the September trajectories from Longview C19. Most of the trajectories approach from the north and east due to the changing season creating in an increase in frontal passages. The majority of the exceedance-ozone trajectories may approach from the left due to the local influence of industry around the Houston ship channel, located on the left side of the line approximately 10 km southeast of Aldine C8.

The number of trajectories in all four groups in the September 1996-1999 trajectories from Longview C19 and the total number of trajectories for September 1996-1999 from Aldine is similar, 2737 and 2723 respectively. The numbers are not the same because the trajectories from times when ozone data was not recorded at the station cannot be

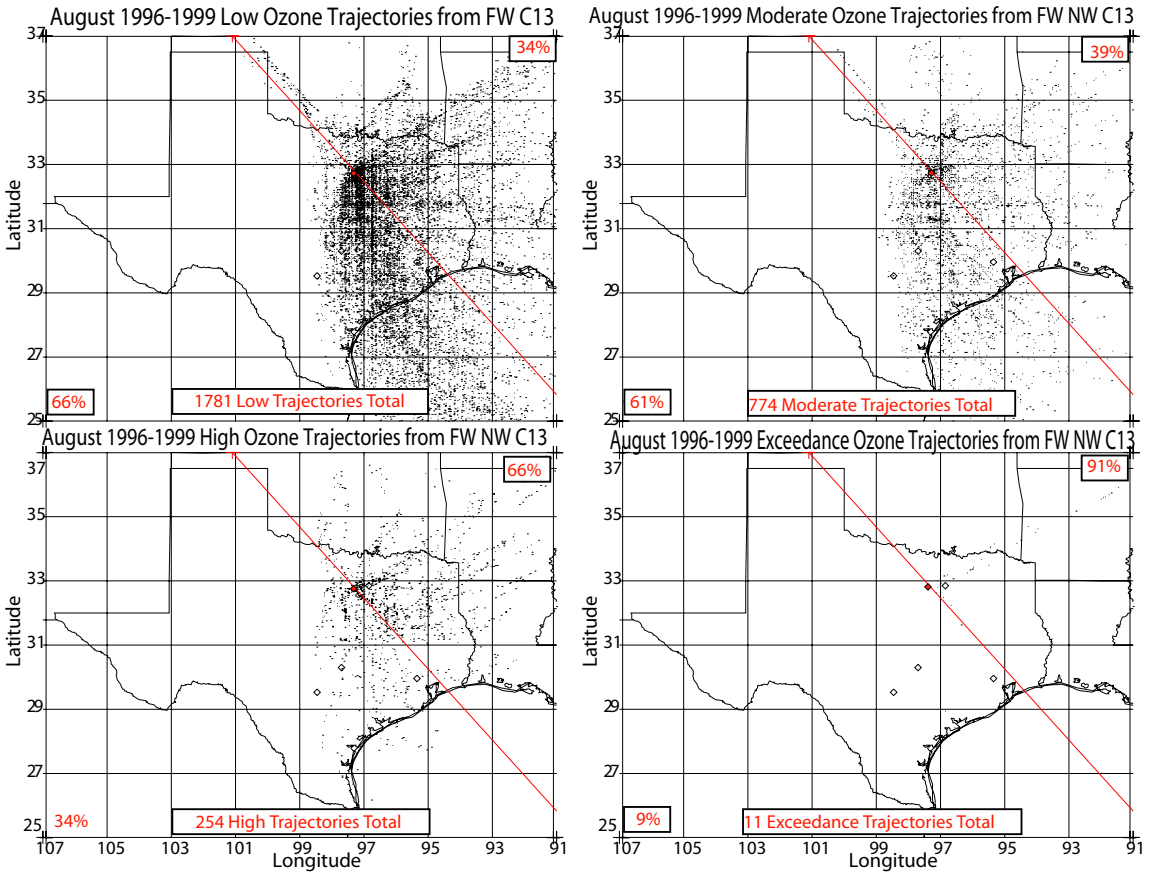

Fig. 15. Forty-eight-hour back trajectories for low, moderate, high, and exceedance ozone measurements at Fort Worth Northwest C13 during August 1996–1999.

included. However, there are 1959 low-ozone trajectories from Aldine and only 1623 low-ozone trajectories from Longview C19, a difference of 336 or 9% of the total number of low-ozone trajectories from both stations. In contrast, there are 578 moderate-ozone trajectories in Aldine and 974 in Longview C19, a difference of 396 or 25% of the total number of moderate-ozone trajectories for both stations. This disparity reflects the impact of the relatively clean air from the Gulf on ozone values at Aldine C8. While the air arriving from the south at Aldine C8 is newly off the Gulf, the air arriving at Longview C19 from

Table IX. Percentages of low, moderate, high, and exceedance ozone trajectories that come from each side of the red line in Figure 16 for Aldine C8 during September 1996–1999.

Site: Aldine C8, September

Category	Left side	Right side	Number
Low	31%	69%	1959
Moderate	22%	78%	578
High	30%	70%	155
Exceedance	58%	42%	31
Total	29%	71%	2723

the south has traveled over 300 km of land, resulting in fewer low-ozone trajectories and more moderate-ozone trajectories for Longview C19 when compared to Aldine C8.

6. Synoptic analysis

Synoptic conditions for the three-day period surrounding exceedances are determined from plots of geopotential height made using NCEP Reanalysis data. Additionally, surface meteorological plots created by Unisys Weather are studied to evaluate the synoptic situation. The 48-hour backward trajectories computed from the 5 selected CAMS stations at the time of each exceedance using NCEP Reanalysis winds are studied as well. The synoptic plots, backward station trajectories, and ozone values are compared to determine what conditions are prevalent when ozone exceedances occur. Similarly to the CAMS Lagrangian trajectories, the ozone exceedances occurring in July, August or September from 1996-1999 at Longview C19 and August of 1996–1999 at Tyler Airport C86 are investi-

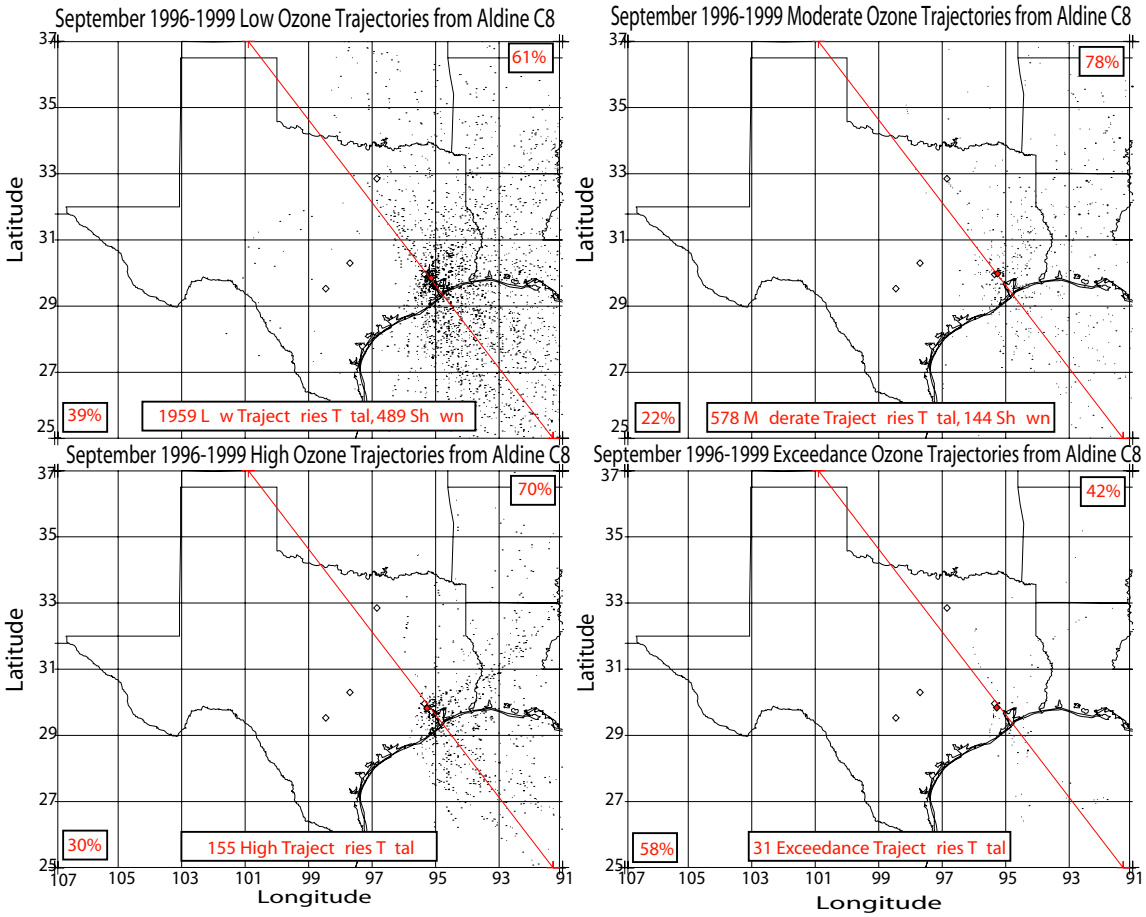

Fig. 16. Forty-eight-hour back trajectories for low, moderate, high, and exceedance ozone measurements at Aldine C8 during September 1996–1999.

gated, as well as the exceedances at Cypress River C50 in July 2000. Details of the ozone exceedances occurring at these 5 stations in the summer months from 1996–2000 are referred to as the event numbers shown in Table 2.

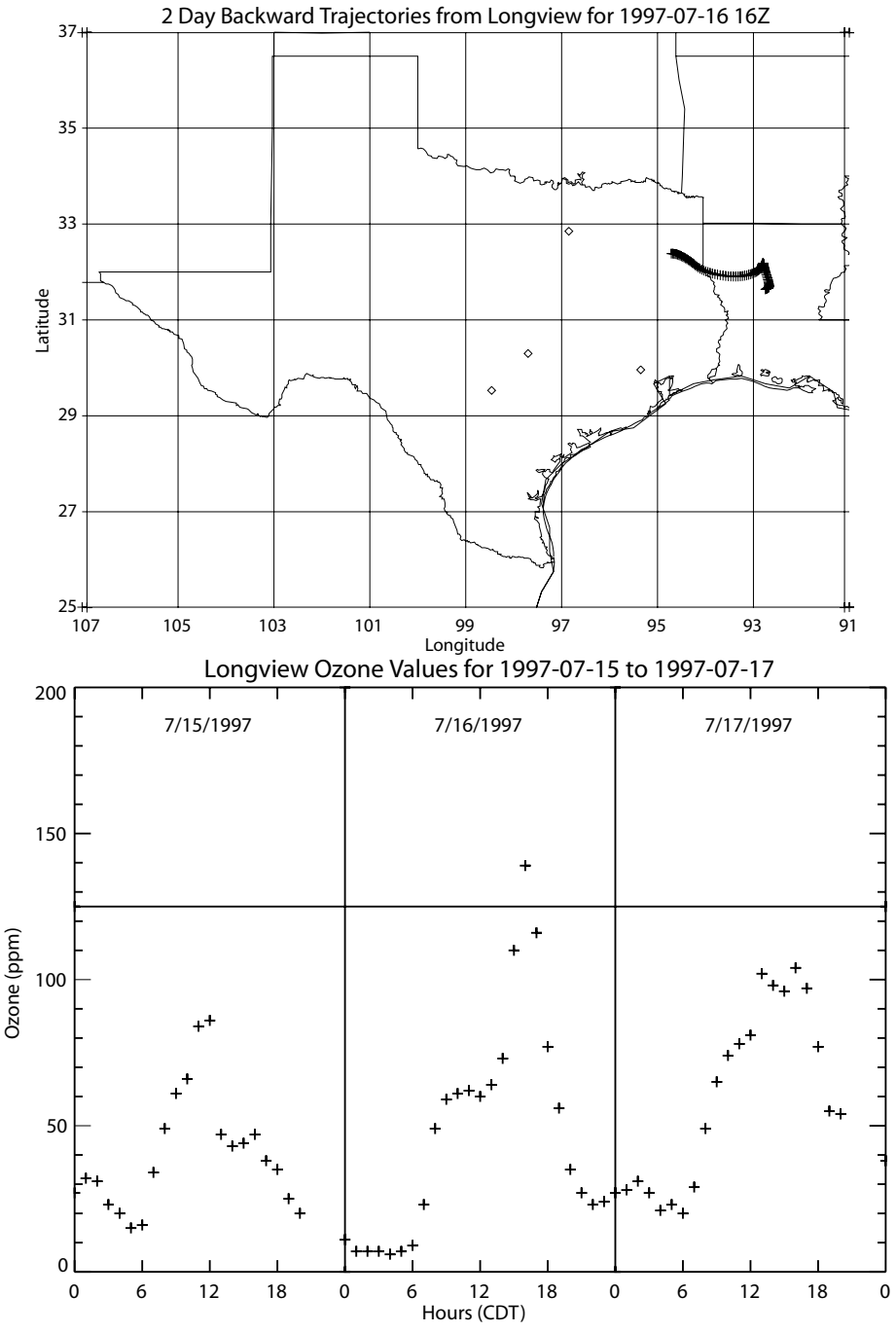

Fig. 17. 48-hour backward trajectory for Event 1. Ozone values for 1997-07-15–1997-07-17 are also shown.

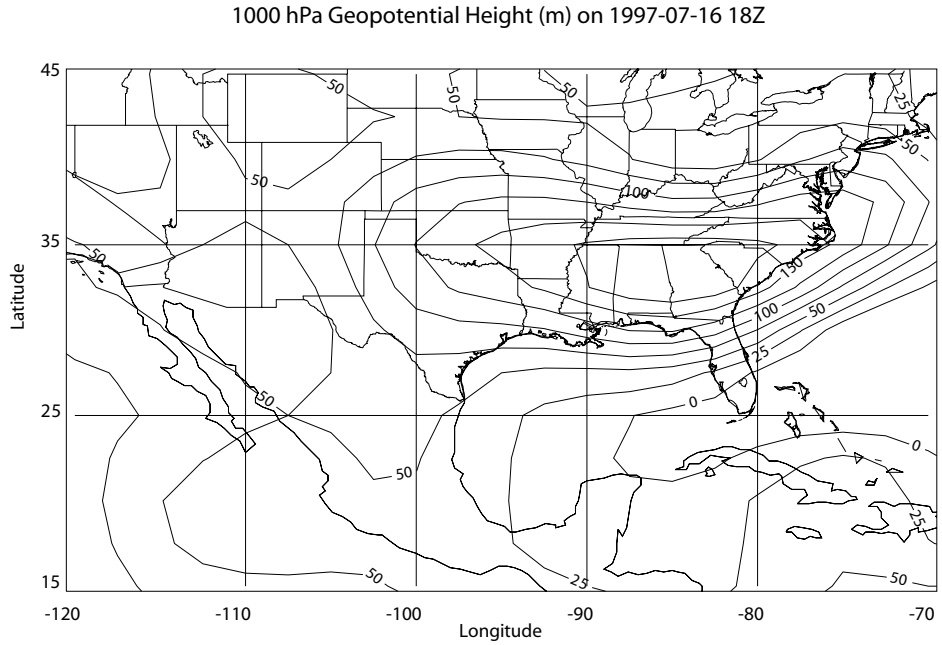

Surface Plot for 1997-07-15 12Z provided by Unisys Corporation, Unisys Weather Information Services

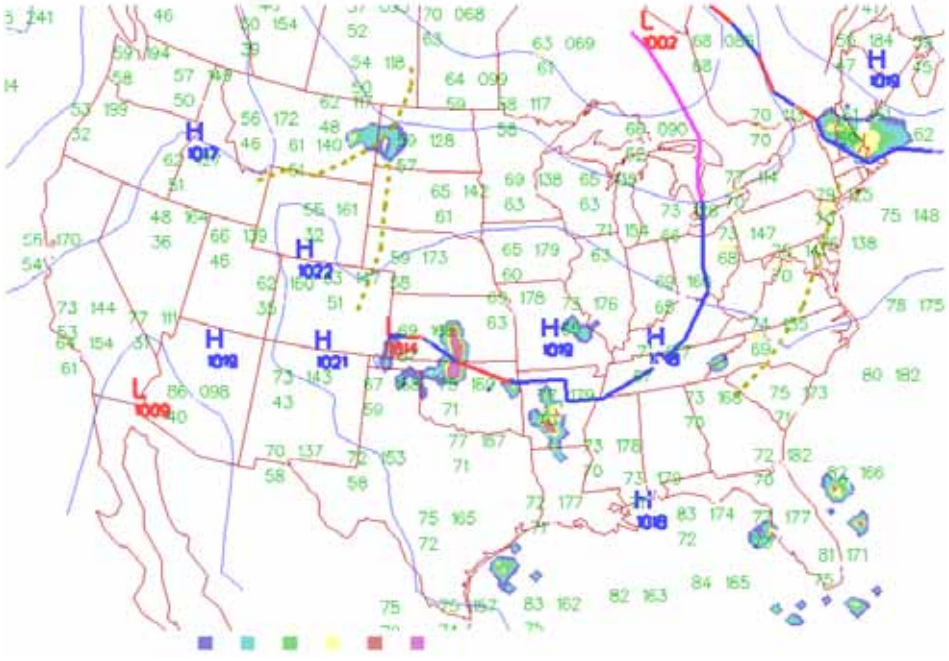

Fig. 18. Geopotential height in m at 1000 hPa on 1997-07-16 at 18Z and a plot of surface weather on 1997-07-15 at 12Z provided by Unisys Corporation, Unisys Weather Information Services.

a. Event 1: Longview C19, 1997-07-16

In Event 1 Longview, Texas, experienced an ozone exceedance on July 16, 1997, at 16Z. The 48-hour backward trajectory from Longview at the time of the exceedance shown in Figure 17 reveals that 48 to 36 hours before reaching Longview the parcel was over central Louisiana moving slowly north. On July 15 at 4Z the parcel abruptly changed direction, moving southwest. Over the next 24 hours the winds rotated from northeast to southeast and the parcel moved northwest until it arrived in Longview. Figure 18 shows the geopotenial height and synoptic conditions near the time of the exceedance.

Initially the parcel experienced southerly flow associated with the Bermuda High. Approximately 36 hours before the parcel arrived in Longview, a cold front passed through central Louisiana causing winds to abruptly shift to the northeast. As the front passed and the parcel moved south and west it was influenced by the area of high pressure behind the cold front, accounting for the clockwise motion of the trajectory. The frequent direction change resulted in a trajectory that covered little distance in the 48 hours prior to its arrival in Longview. The stagnant winds and clear skies associated with high pressure contributed to an ozone level of 139 ppb at 16Z in Longview, 14 ppb over the one-hour standard.

b. Event 2: Longview, TX, 1998-08-16

In Event 2 Longview exceeded the one-hour ozone standard again on August 16, 1998, at 19Z with a value of 127 ppb. The 48-hour backward trajectory in Figure 19 shows very stagnant flow, with the trajectory moving less than 250 km overall. A strong high, shown in Figure 20, was centered over northeast Texas on the 16th with a geopotential height of almost 175 m at the 1000 mb level. The high pressure caused calm winds at the surface, clear skies, and a high temperature of 92 F. The abundant sunlight and lack of mixing led to an ozone exceedance.

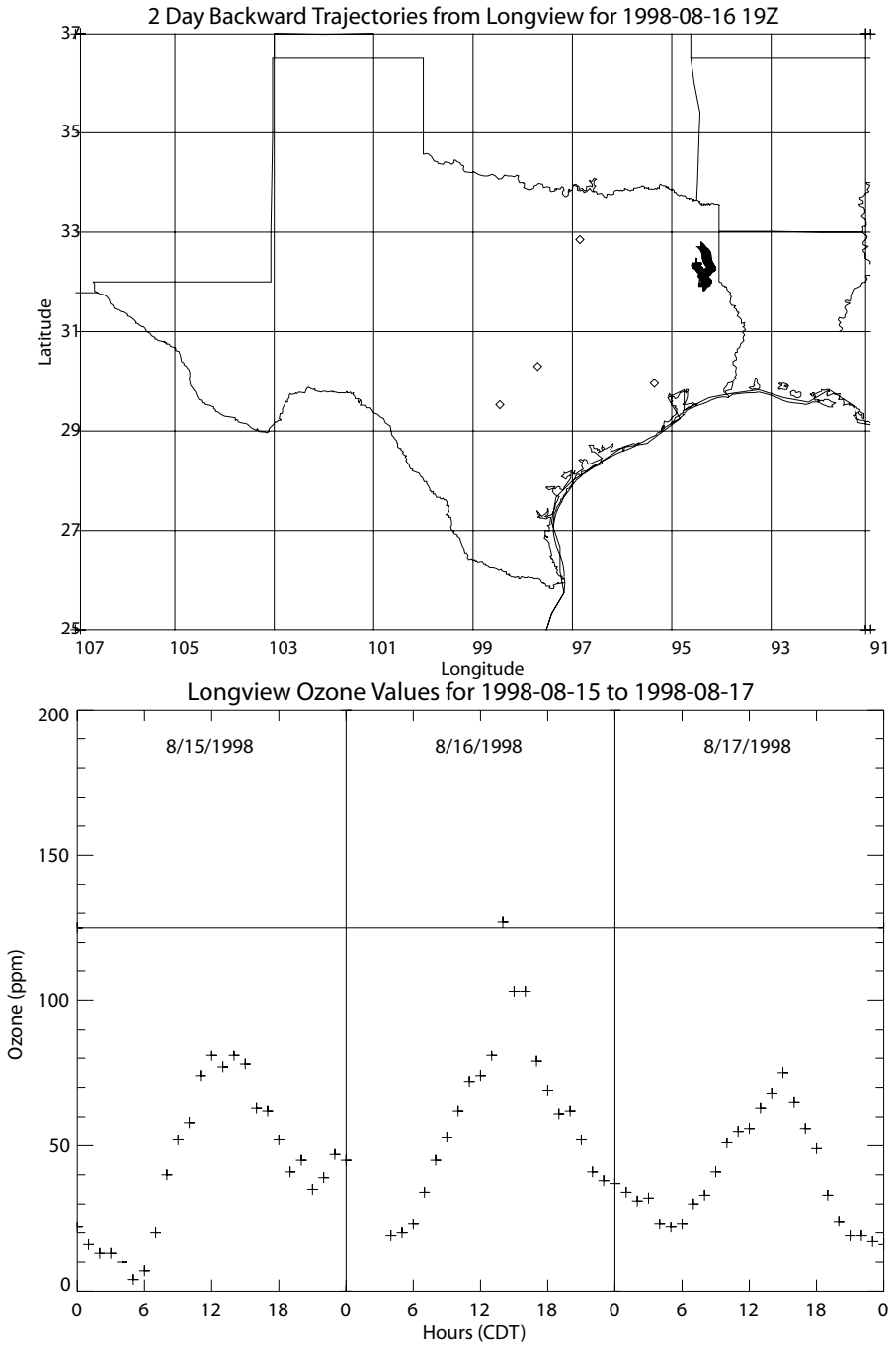

Fig. 19. 48-hour backward trajectory for Event 2. Ozone values for 1998-08-15–1998-08-17 are also shown.

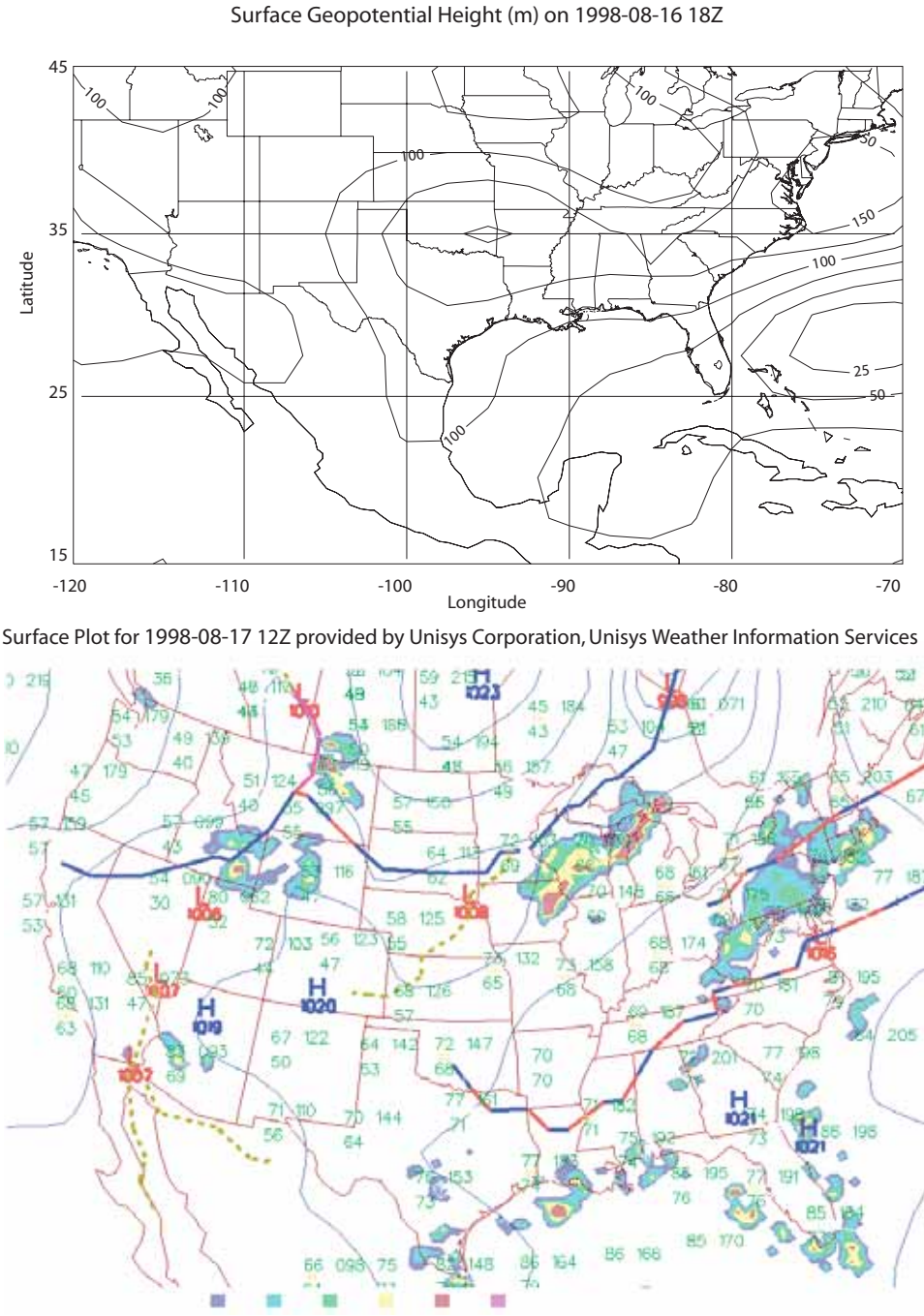

Fig. 20. Geopotential height in m at 1000 hPa on 1998-08-16 at 18Z and a plot of surface weather on 1998-08-17 at 0Z provided by Unisys Corporation, Unisys Weather Information Services.

c. Event 3: Longview, TX, 1998-08-28

Over a week later in Event 3 on August 28, 1998, at 19Z, Longview experienced another exceedance with an ozone value of 129 ppb. The 48-hour backward trajectory from Longview shown in Figure 21 initially showed the parcel moving northwest, then changing direction to move northeast before shifting to the northwest roughly 12 hours before arriving. From 48 to 12 hours before arriving the parcel was influenced by southwesterly flow into a warm front associated with a low centered in northeast Missouri, shown in Figure 22. Then on the 28th around 7Z the trajectory began to be influenced by the cold front approaching from the northwest.

The cold front arrived in Longview at 23Z, as shown in Figure 22, bringing light winds and showers. The exceedance was a result of light winds, abundant sunlight, and a high temperature of 101F. Additionally, air from both Houston and the Dallas/Fort Worth area likely influenced Longview, from the southeasterly and northwesterly flow, respectively. Ozone values remained high the next day, peaking with a value of 123 ppb at 17Z. The passage of the front brought air that had been moving north out of Texas for several days in the typical summertime southerly flow back into the Longview area within 18 hours. The lifetime of surface ozone is generally a few days, so a significant portion of the ozone was brought back to the Longview area before it was depleted, contributing to an ozone level of 123 ppb on the 29th.

d. Event 4: Longview, TX, 1998-09-03

In Event 4 at 22Z on the 3rd ozone reached 125 ppb in Longview. The backward trajectory in Figure 23 reveals that up to 6 hours before arriving the flow was from the northeast, due to a small area of high pressure over Arkansas ahead of a trough approaching from the west.

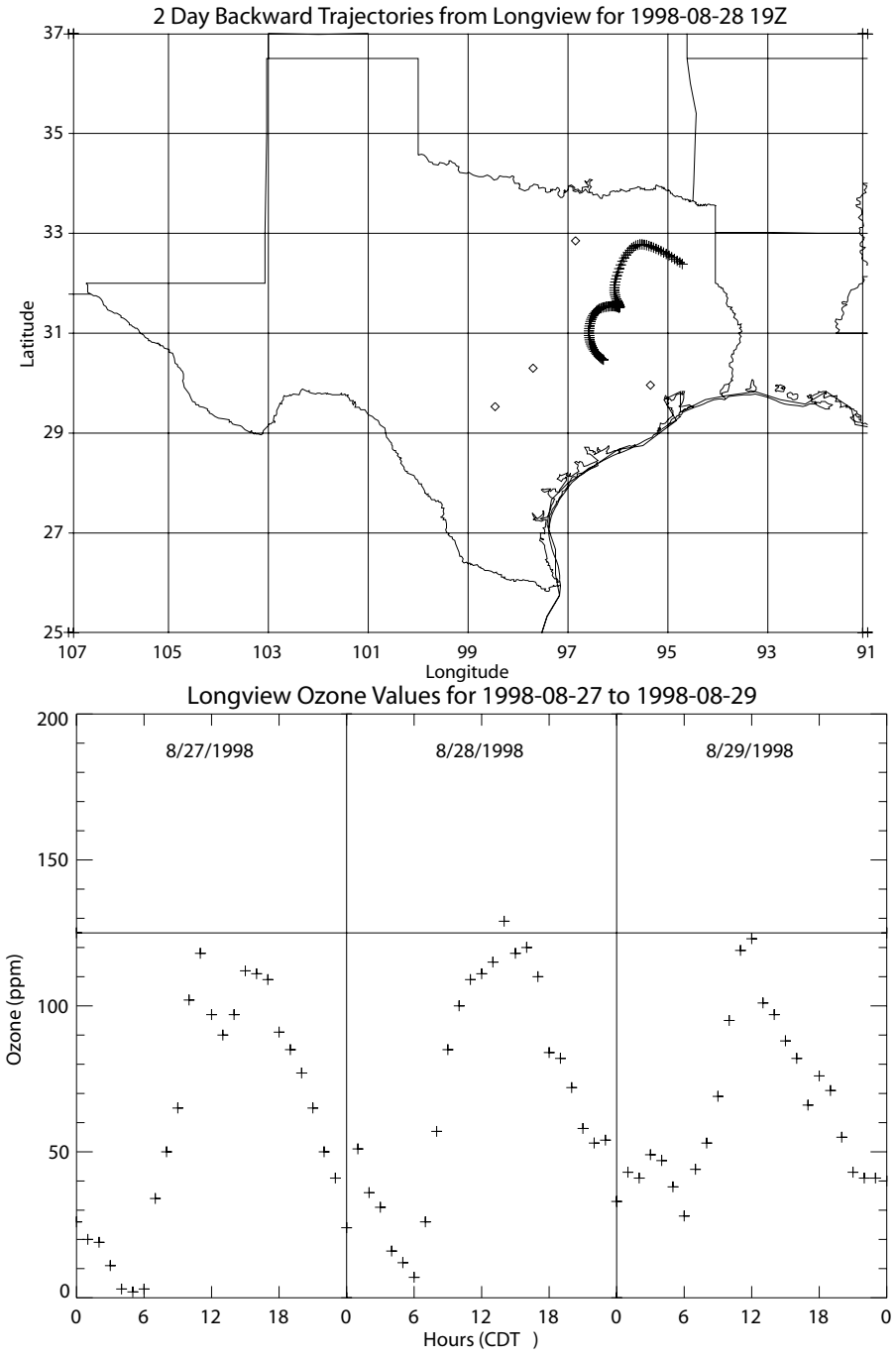

Fig. 21. 48-hour backward trajectory for Event 3. Ozone values for 1998-08-27–1998-08-29 are also shown.

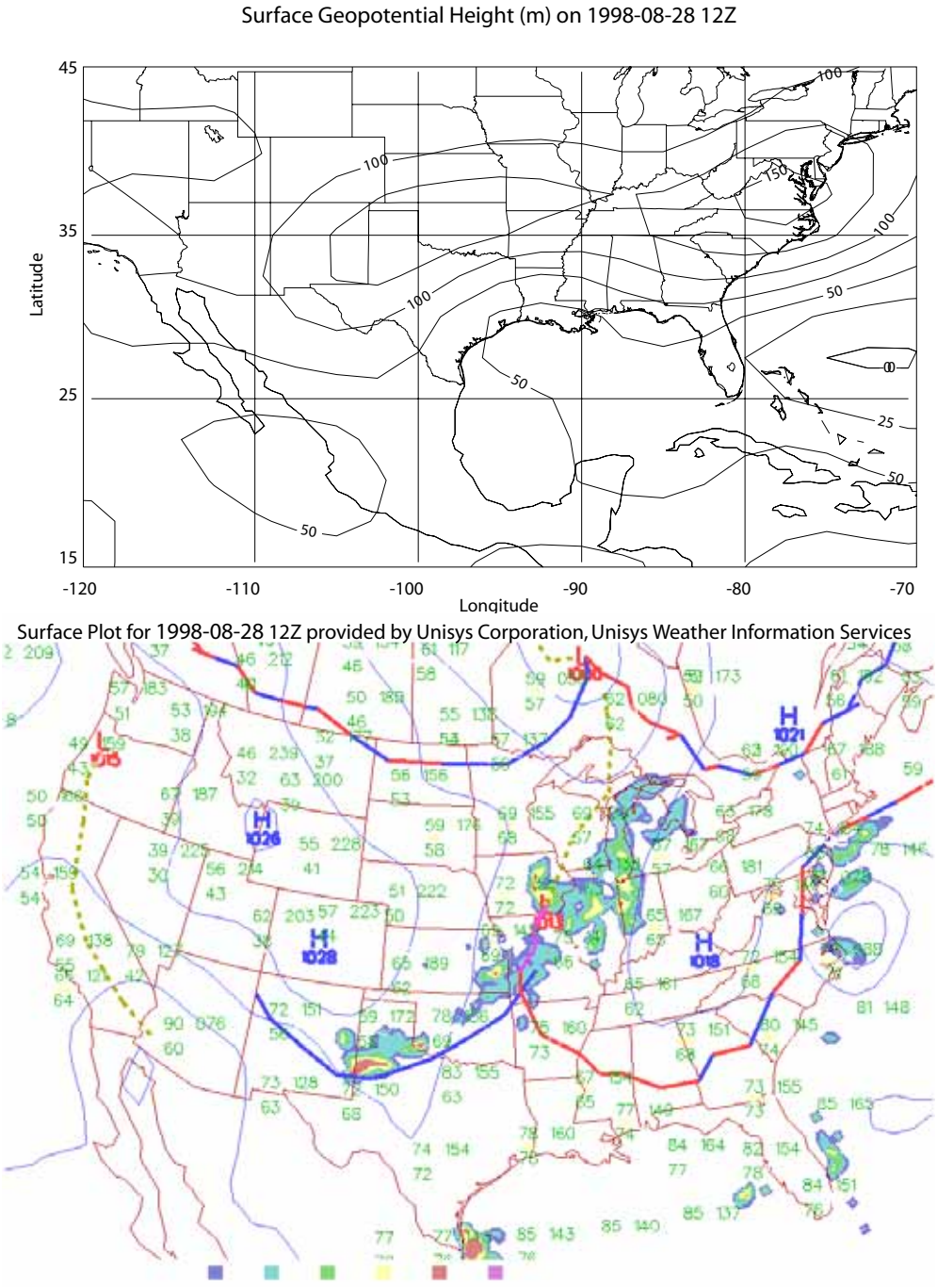

Fig. 22. Geopotential height in m at 1000 hPa on 1998-08-28 at 18Z and a plot of surface weather on 1998-08-29 at 0Z provided by Unisys Corporation, Unisys Weather Information Services.

Around 16Z the trajectory began to be influenced by the trough shown in Figure 24, and the parcel turned clockwise to move north. No precipitation was associated with this trough. A temperature of 98F and sunny skies in combination with a relatively stagnant trajectory due to the change in wind direction led to an exceedance.

e. Events 5 and 6: Houston, TX, 1998-09-03 and 1998-09-04

Two areas in east Texas experienced ozone exceedances beginning on September 3, 1998. In Event 5 Aldine, a station 10 km southwest of downtown Houston experienced exceedances on September 3, 1998, from 17-20Z, as well as on the following day in Event 6 from 2-3Z and 17-19Z. The backward trajectories from Aldine in Figure 25 resemble the one from Longview. They parcels initially move southwest before negotiating a clockwise turn. This clockwise motion becomes more pronounced the later the trajectory's arrival time. For example, the trajectories in Event 5 are moving west before arrival, while those in Event 6 from 2-3Z move west-northwest, and finally those from 17-19Z move north-northeast.

The later trajectories are influenced by the passage of the trough, shown in Figure 26, farther back in time, giving it more time to affect their motion. In fact, the strong clockwise motion of the parcels in Event 6 is due to an area of high pressure in southeast Texas that forms as the trough stalls. Ozone values were higher in Event 6 due to the parcels' slower clockwise loop around southeast Texas' industrial gulf coast, with three hours of exceedance-level values peaking at 155 ppb at 19Z. A less stagnant backward trajectory for Event 5 produced a lower peak ozone value of 143 ppb at 20Z, and a total of four hours of ozone values greater than 125 ppb.

f. Event 7: Fort Worth, TX, 1999-08-03

Ozone exceedances were widespread, impacting Fort Worth, Longview, and Tyler, Texas, from August 3, 1999, to August 5, 1999 in Events 7-11. To begin, in Event 7 Fort Worth experienced an ozone exceedance of 132 ppb on August 3 at 20Z. The 48-hour backward trajectory for Event 7 in Figure 27 undulates between 12 hours of parcel motion to the northwest, followed by 12 hours of southwest motion, throughout the 48 hours

shown. The parcel's northwesterly and southwesterly motion is due to its path north and south of a slow-moving approaching cold front shown in Figure 28. In the days before the exceedance central Texas experienced typical summertime southerly flow. The overall motion of the parcel to the southwest caused the air that had been previously transported northward in this southerly flow to be cycled south back into Texas. Temperature peaked at 98F at the time of the exceedance. The air that thad been transported into the area from the northeast likely contained ozone precursors after traveling over many kilometers of populated and industrialized land in the midwest. Air that had traveled north in the summertime southerly flow over Texas and the western Gulf coast states in advance of the front was also transported back into the region. Sunshine and light winds in combination with the cyclical transport of air north and then southwest across Texas were likely the contributing factors behind this exceedance.

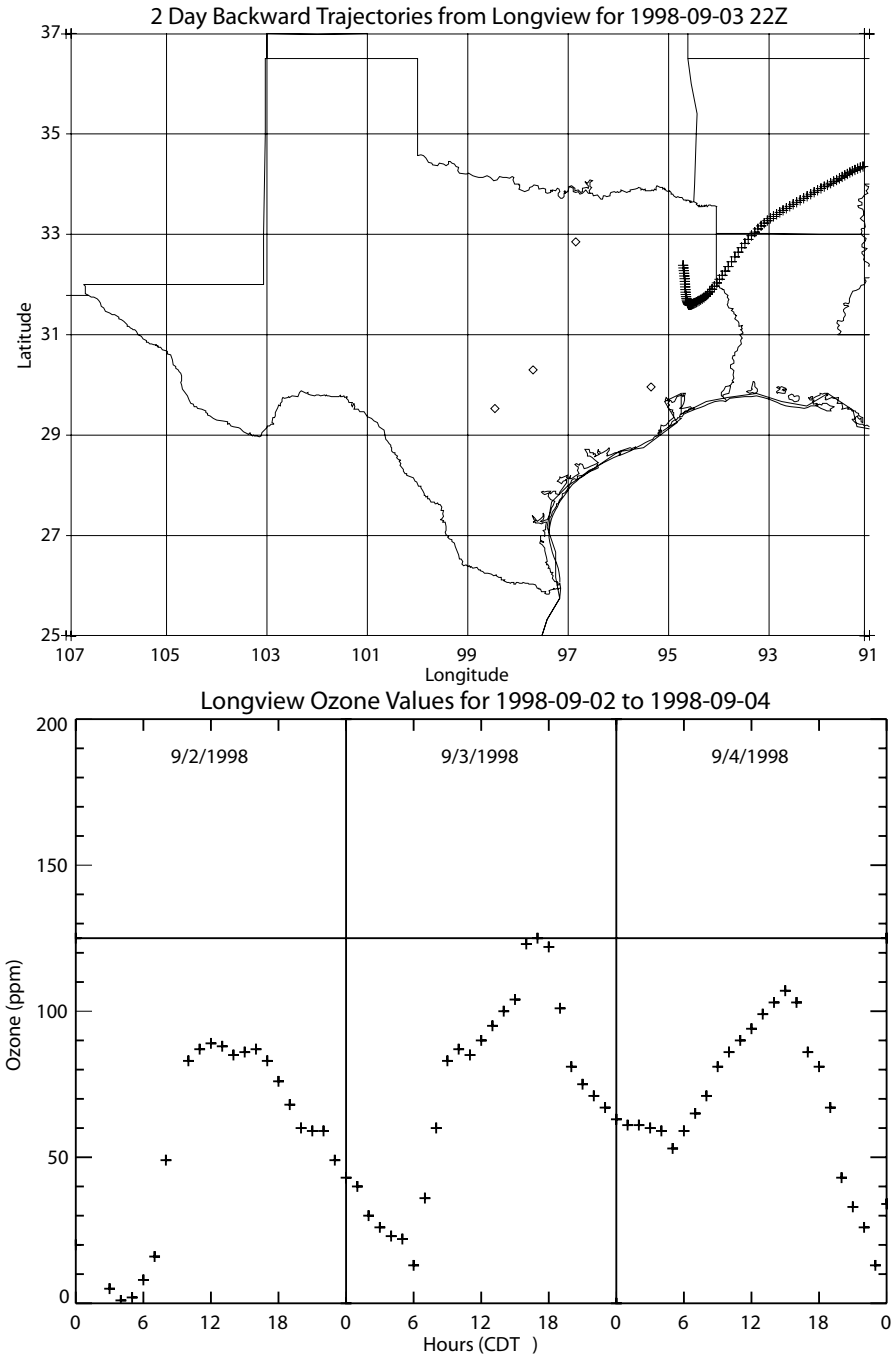

Fig. 23. 48-hour backward trajectory for Event 4. Ozone values for 1998-09-03–1998-09-05 are also shown.

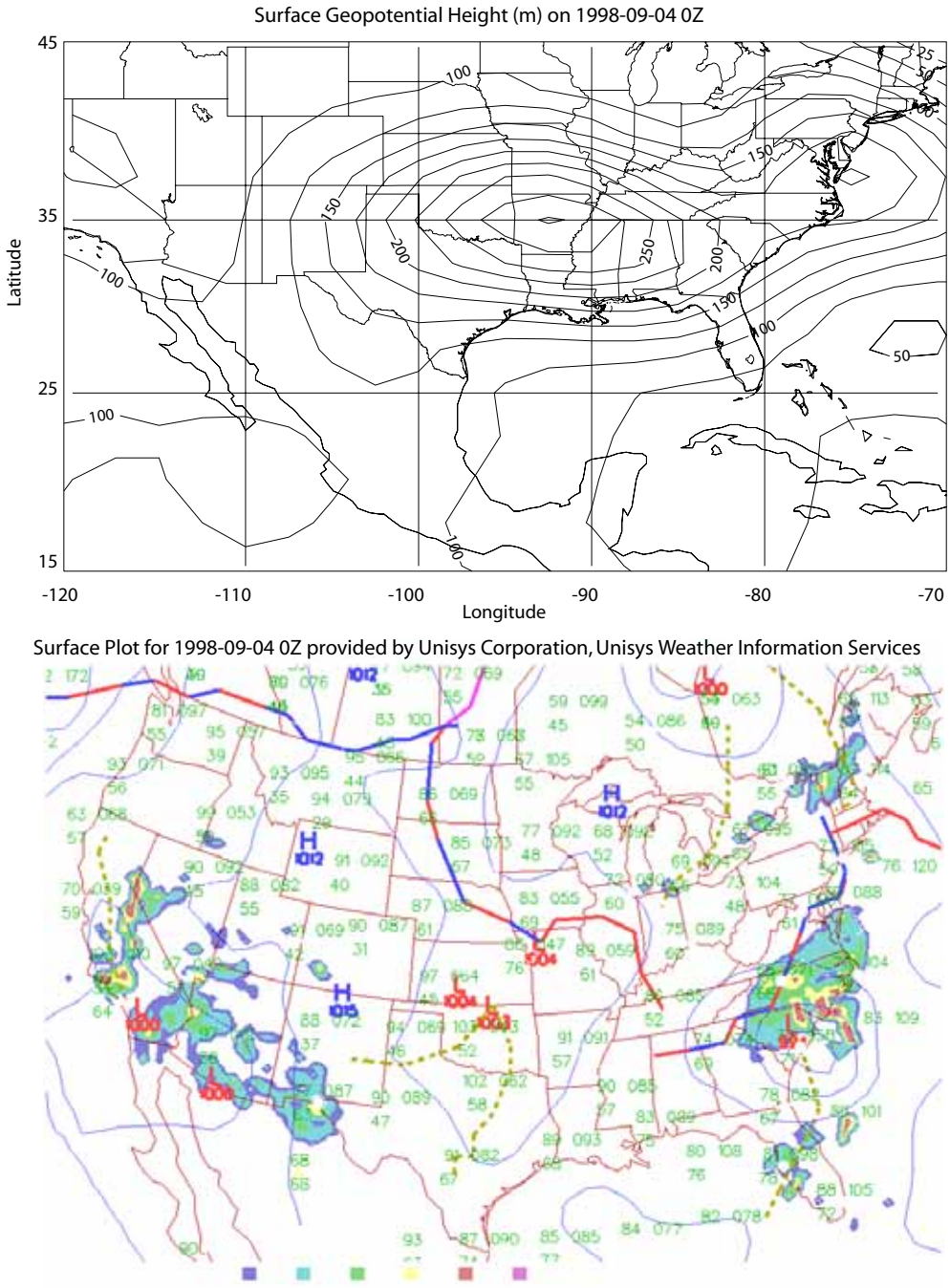

Fig. 24. Geopotential height in m at 1000 hPa on 1998-09-04 at 0Z and a plot of surface weather on 1998-09-04 at 0Z provided by Unisys Corporation, Unisys Weather Information Services.

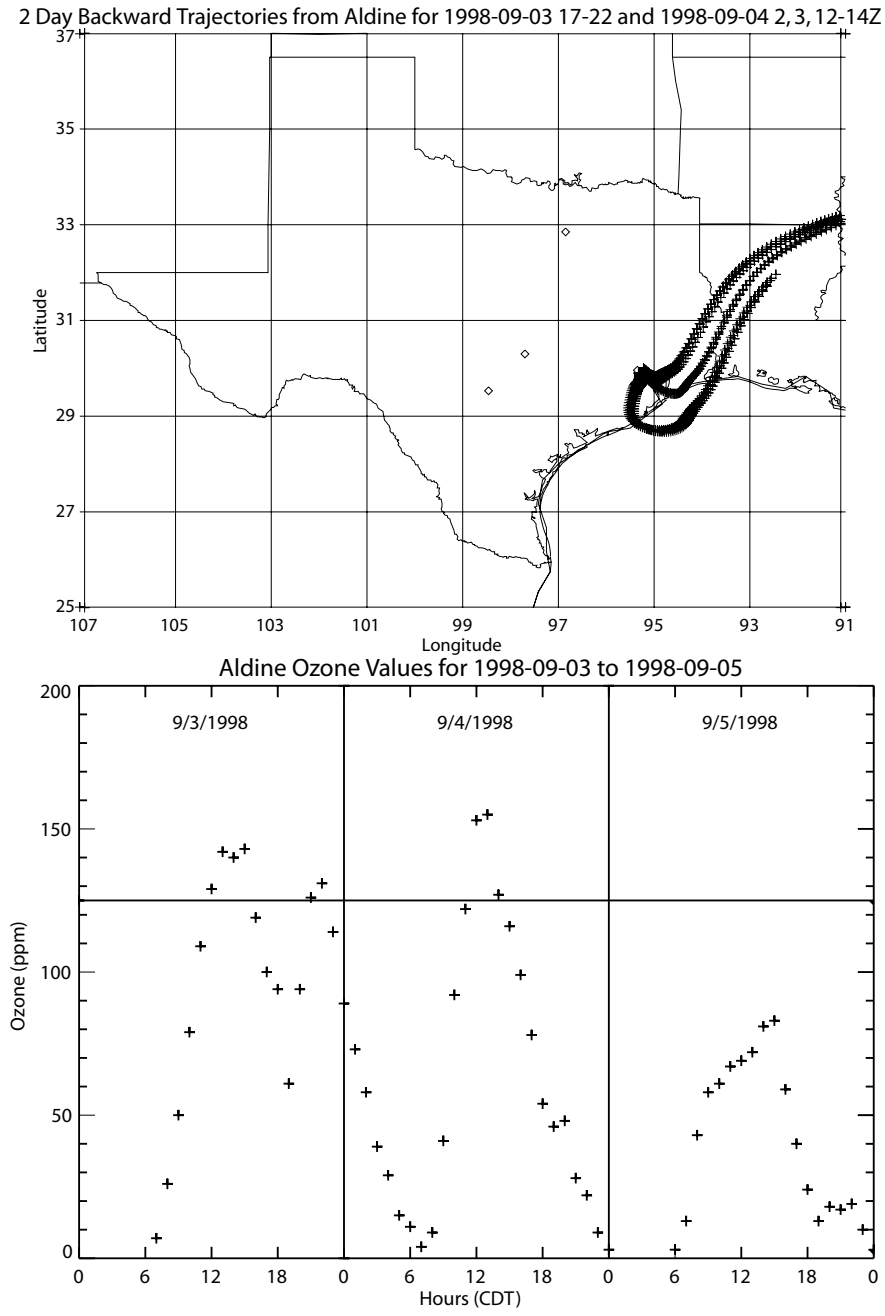

Fig. 25. 48-hour backward trajectories for Events 5 and 6. Ozone values for 1998-09-03–1998-09-05 are also shown.

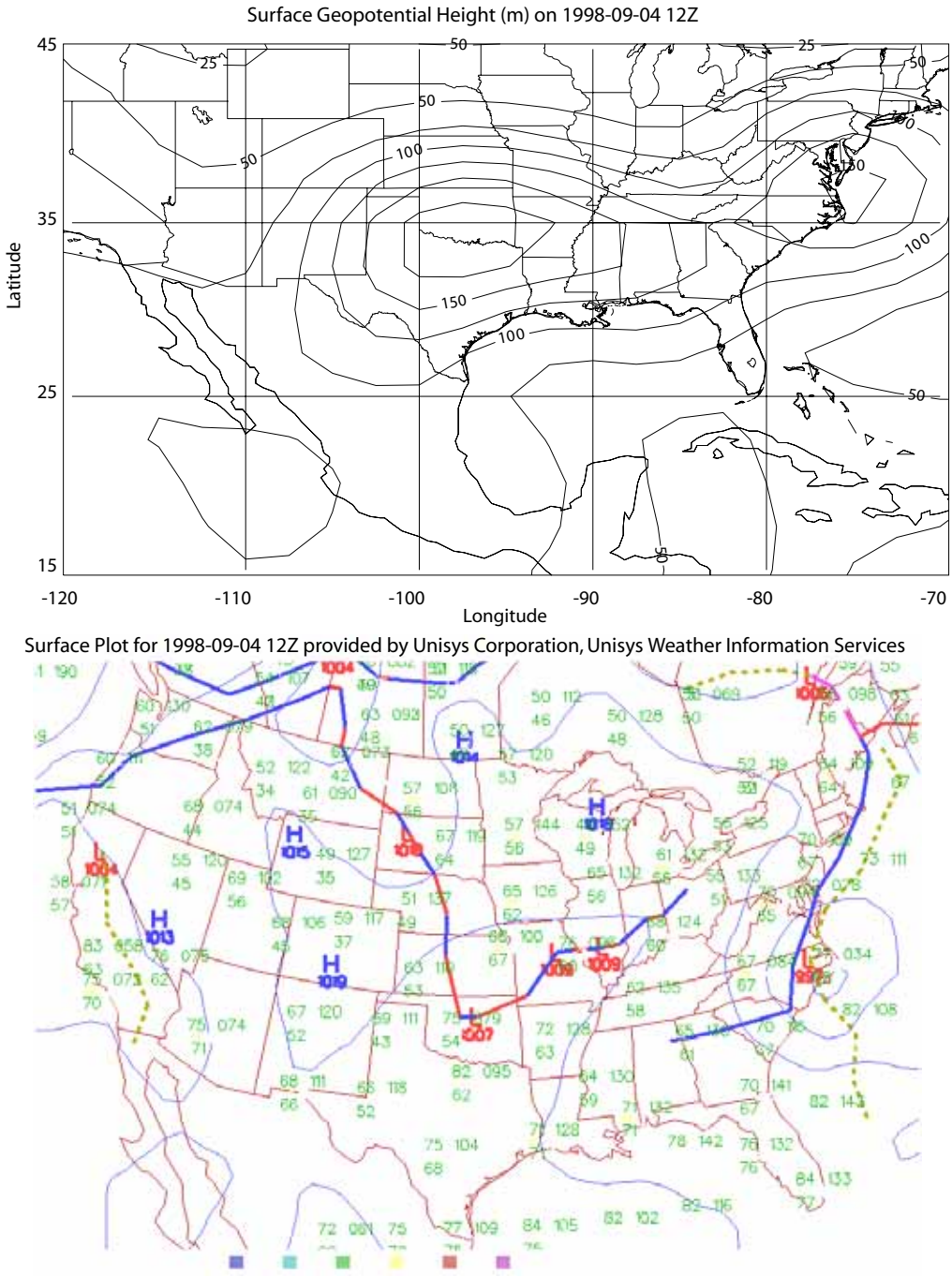

Fig. 26. Geopotential height in m at 1000 hPa on 1998-09-04 at 12Z and a plot of surface weather on 1998-09-04 at 12Z provided by Unisys Corporation, Unisys Weather Information Services.

g. Event 8: Fort Worth, TX, 1999-08-04

The synoptic conditions were the same for exceedances occurring the next day in Fort Worth during Event 8. Event 8 consisted of one-hour ozone exceedances from 18-21Z peaking at 164 ppb at 19Z. During Event 8 north Texas experienced mostly cloudy skies with scattered precipitation, light winds, and temperatures in the mid-nineties. The backward trajectory shown in Figure 27 shows consistent parcel motion to the southwest. Again, the transport of air southwestward into Texas that had previously been moved north across Texas in the southerly flow before the frontal passage likely contributed to the exceedance.

h. Event 9: Fort Worth, TX, 1999-08-05

In Event 9 on August 5th, ozone exceedances persisted in Fort Worth, occurring from 18-21Z and peaking at 154 ppb at 20Z. North Texas was experiencing widely scattered showers and temperatures in the upper nineties. Trajectories for Event 9 in Figure 27 show southwesterly parcel motion for all but the last twelve hours, during which the parcels move west. The cold front stalls across Fort Worth from the 3rd at 0Z, shown in Figure 28, to the 5th at 0Z. An area of high pressure develops in northeast Texas around 12Z on the 5th in the wake of the trough, inducing easterly winds in Fort Worth. The ozone-laden air transported southwest into the area over the previous days by the front, in combination with the presence of high pressure over the area after the front stalled, contributed to the exceedances.

i. Event 10: Longview, TX, 1999-08-04

In Event 10 Longview experienced an ozone value of 132 ppb at 16Z. The backward trajectory in Figure 29 shows the parcel consistently moving southwest since it arrived after those shown in Event 7 arriving in Fort Worth, and was influenced by the northeasterly flow

behind the cold front throughout the 48-hour period. As shown in Figure 30, north Texas experienced mostly cloudy skies with scattered precipitation, light winds, and temperatures in the mid-nineties. The forces behind the exceedance are the same as those behind the exceedances in Fort Worth during Events 7–9, ozone-laden air from Texas and the northeast U.S. is brought southwest in Texas.

j. Event 11: Tyler, TX, 1999-08-05

In Event 11 Tyler experiences exceedances from 17-21Z with a high value of 127 ppb at 19Z. The 48-hour backward trajectories from Tyler in Figure 31 show the parcels moving consistently to the southwest. As seen in Figure 32, the cold front stalls west of Tyler from the 3rd at 0Z to the 5th at 0Z. An area of high pressure develops in northeast Texas around 12Z on the 5th in the wake of the trough, maintaining northeasterly winds in Tyler. The parcels moving toward Tyler do not move west 12 hours before arrival as they did in Event 9 to Fort Worth, because Tyler is 215 km east of Fort Worth and experiences the northeasterly flow on the east side of the high. Again, the southerly transport of ozone-laden air likely contributed to the exceedance.

k. Event 12: Longview, TX, 1999-08-17

Two weeks after these widespread high ozone values Longview reported exceedances during Event 12, peaking with a value of 134 ppb at 21 and 22Z. 48 to 36 hours before arriving the trajectories shown in Figure 33 were moving southwest, due to flow behind a cold front that passed on the 15th around 12Z. As shown in Figure 34, around 12Z on the 16th an area of high pressure formed behind the cold front over southern Arkansas, with a surface pressure of 1020.6 mb. The high persisted until the trajectories arrived, as seen in

Figure 34, causing a clockwise turn in the parcels' motion. Clear skies, very light winds resulting in a slow-moving trajectory, and a high temperature in the upper nineties coupled with ozone-laden air from the northeast being transported into the area by the southwesterly flow of the cold front led to an exceedance.

l. Event 13: Longview, TX, 1999-09-20

In Event 13, Longview experienced a late-season ozone exceedance of 138 ppb at 16Z. The 48-hour backward trajectory from Longview in Figure 35 reveals that up to 12 hours before arriving the parcel experienced light easterly winds associated with the southern portion of the clockwise circulation around an area of high pressure over the eastern U.S. Around 0Z on the 20th a cold front with a surface pressure of 1005 mb, shown in Figure 36, approached from the west. The trajectory began to show parcel motion to the northwest, under the influence of southeasterly winds on the eastern edge of the counterclockwise circulation around the low. The front eventually passed through Longview 3 hours after the exceedance at 19Z. Longview was experiencing clear skies, wind speeds of 4 m/s, and a temperature of 89F at 16Z. The southeasterly flow likely brought air on its way north-northwestward from Houston into the area. Light winds and ozone-laden air from southeast Texas along with abundant sunlight led to an exceedance.

m. Event 14: Jefferson, TX, 2000-07-16

The only one-hour ozone exceedances recorded at Cypress River C50 occurred on during Event 14. Ozone values were greater than 125 ppb for 3 hours and peaked at 21Z with a value of 148 ppb. The 48-hour backward trajectory in Figure 37 shows steady parcel motion from the south-southwest, with the trajectory passing roughly 50 km to the west of

downtown Houston 24 hours prior to arrival. The surface chart explains that the northward flow was induced by a stalling trough. Almost 48 hours before arrival the trough, shown in Figure 38, ran horizontally across Texas near 31N. The western half of the trough had moved north to 33N 12 hours later, while the location of the eastern half remained constant. The eastern half of the trough also moved north to 33N 24 hours prior to arrival, and remained there until dying out 12 hours later. Cypress River C50 experienced a high temperature of 99 F on July 16 at the time of the exceedance along with calm winds and clear skies. The cyclical motion of the air across Texas, coupled with high temperature, clear skies, and calm winds resulted in an exceedance-level ozone event.

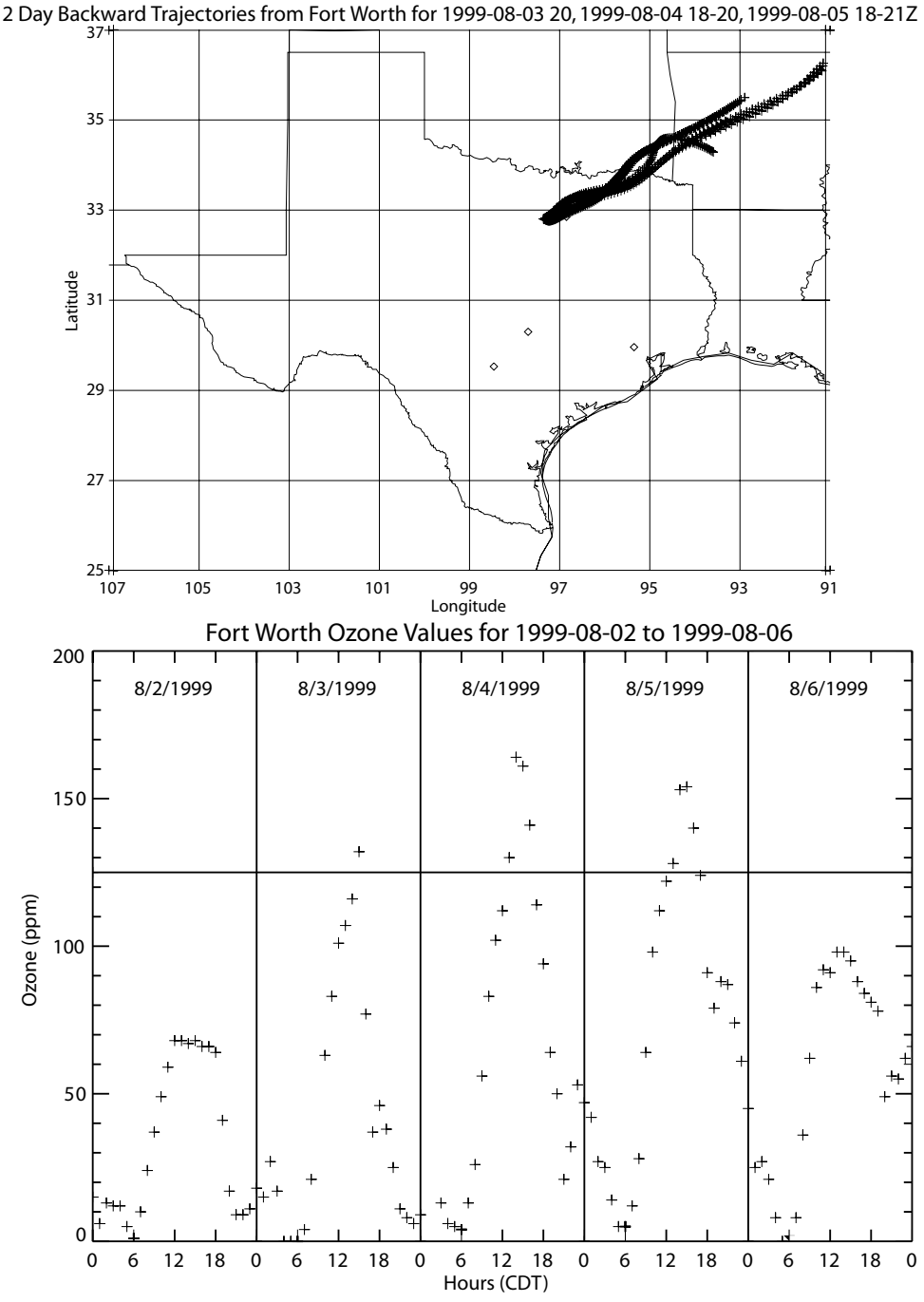

Fig. 27. 48-hour backward trajectories for Events 7-9. Ozone values for 1999-08-02–1999-08-06 are also shown.

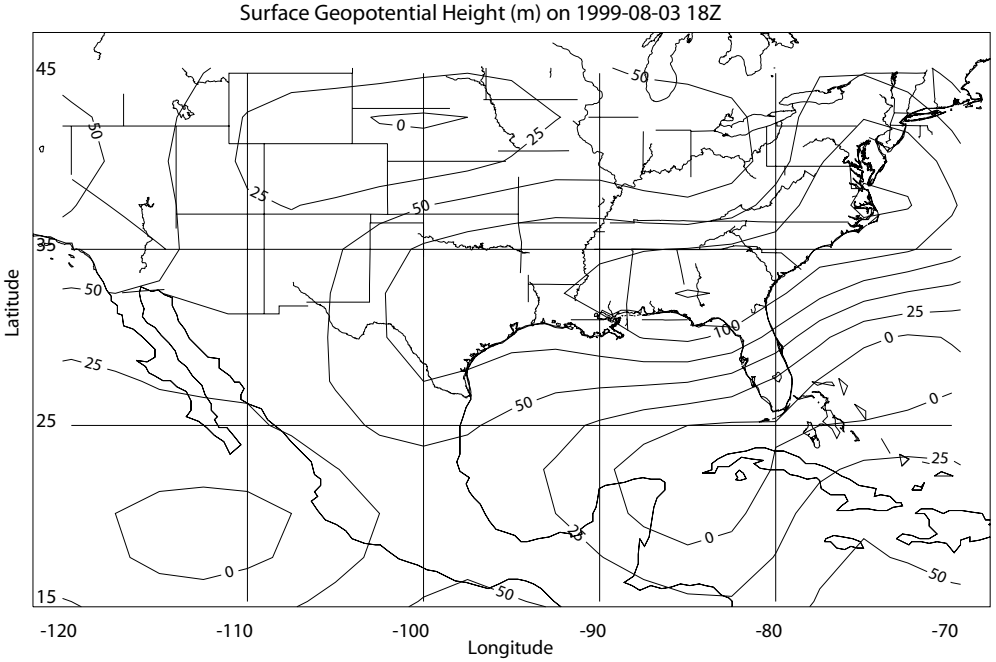

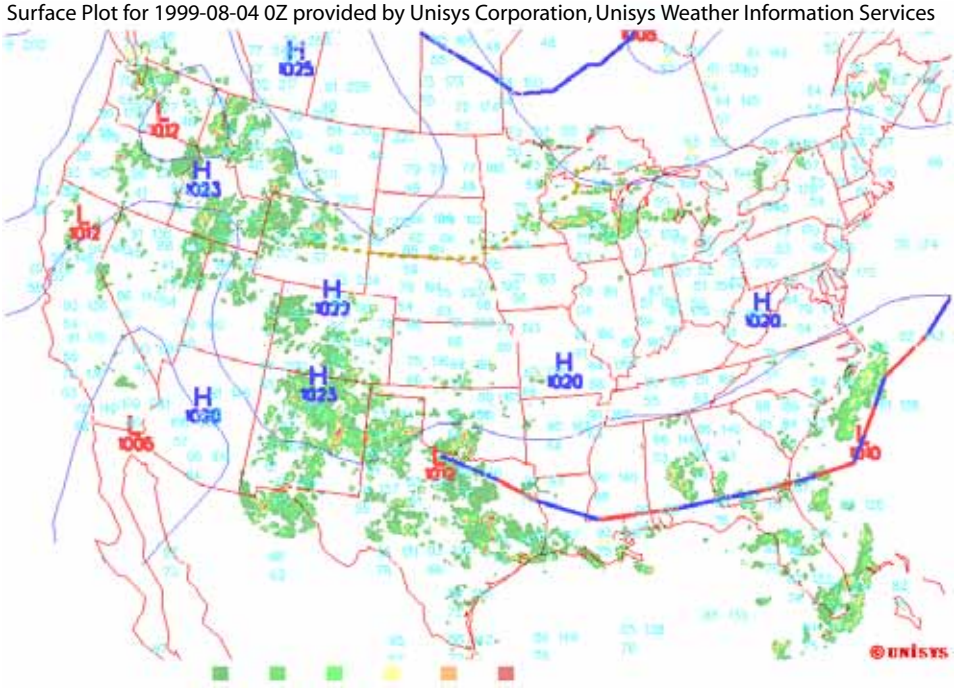

Fig. 28. Geopotential height in m at 1000 hPa on 1999-08-03 at 18Z and a plot of surface weather on 1999-08-04 at 0Z provided by Unisys Corporation, Unisys Weather Information Services.

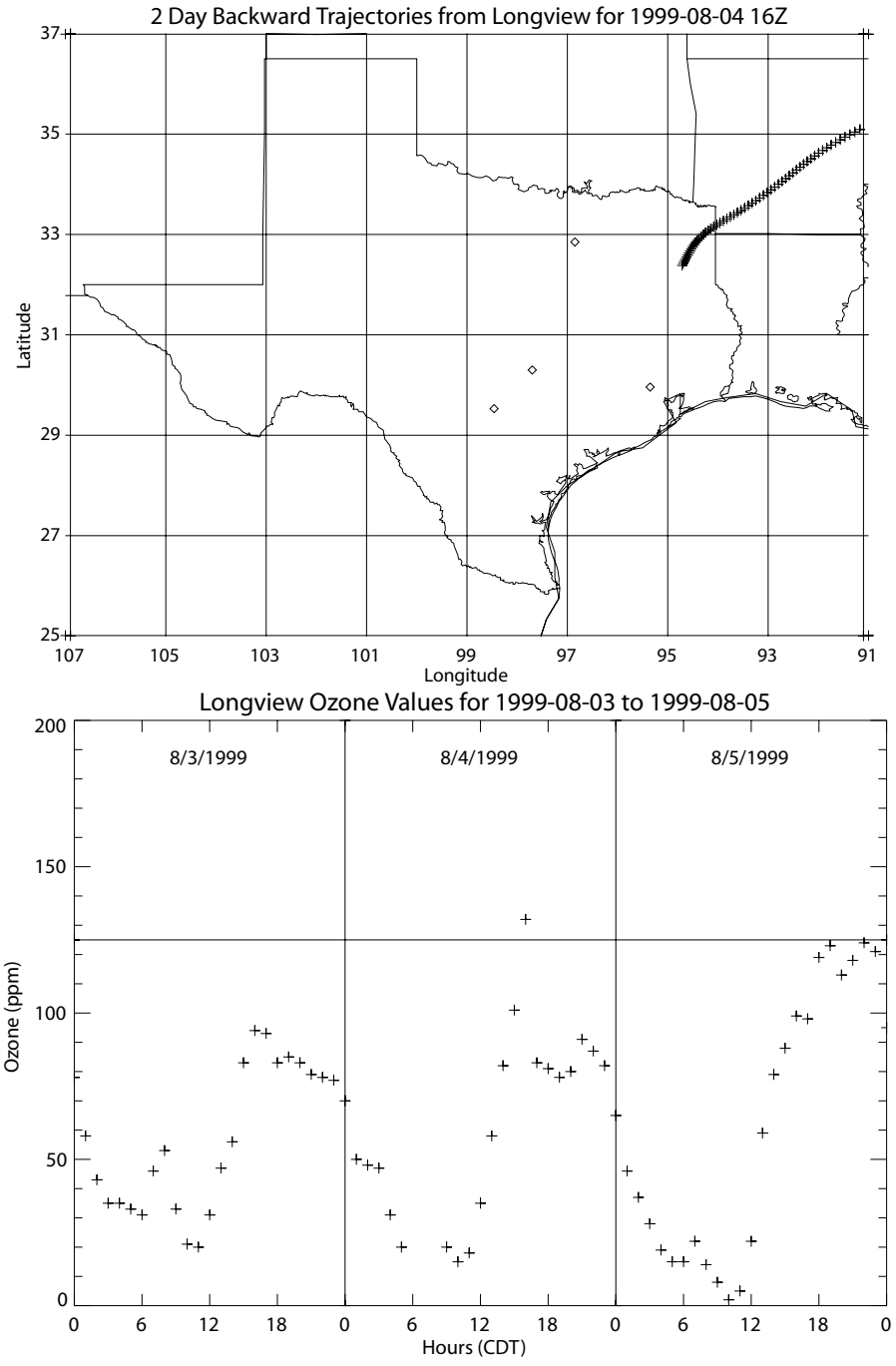

Fig. 29. 48-hour backward trajectory for Event 10. Ozone values for 1999-08-03–1999-08-05 are also shown.

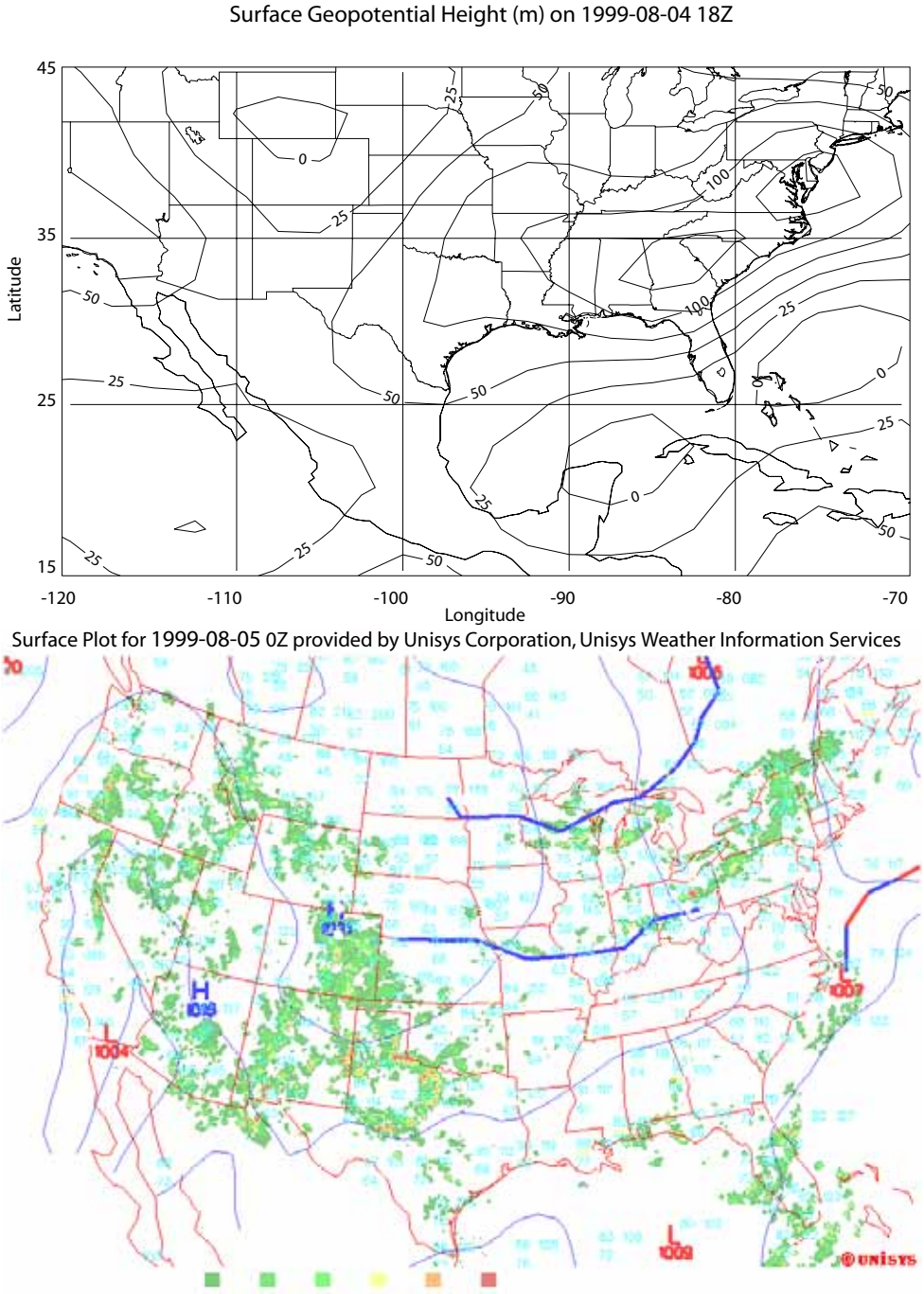

Fig. 30. Geopotential height in m at 1000 hPa on 1999-08-04 at 18Z and a plot of surface weather on 1999-08-05 at 0Z provided by Unisys Corporation, Unisys Weather Information Services.

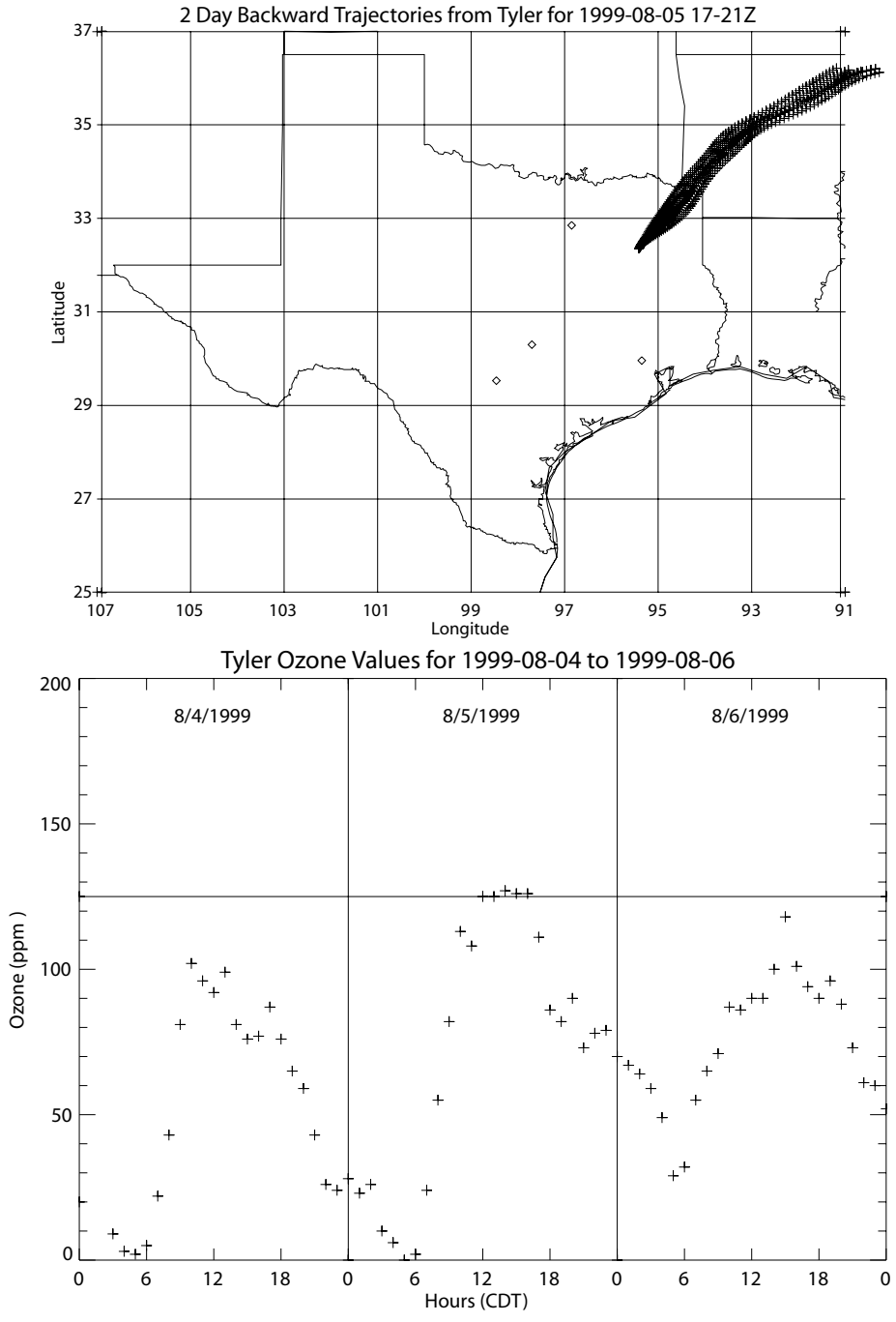

Fig. 31. 48-hour backward trajectories for Event 11. Ozone values for 1999-08-04–1999-08-06 are also shown.

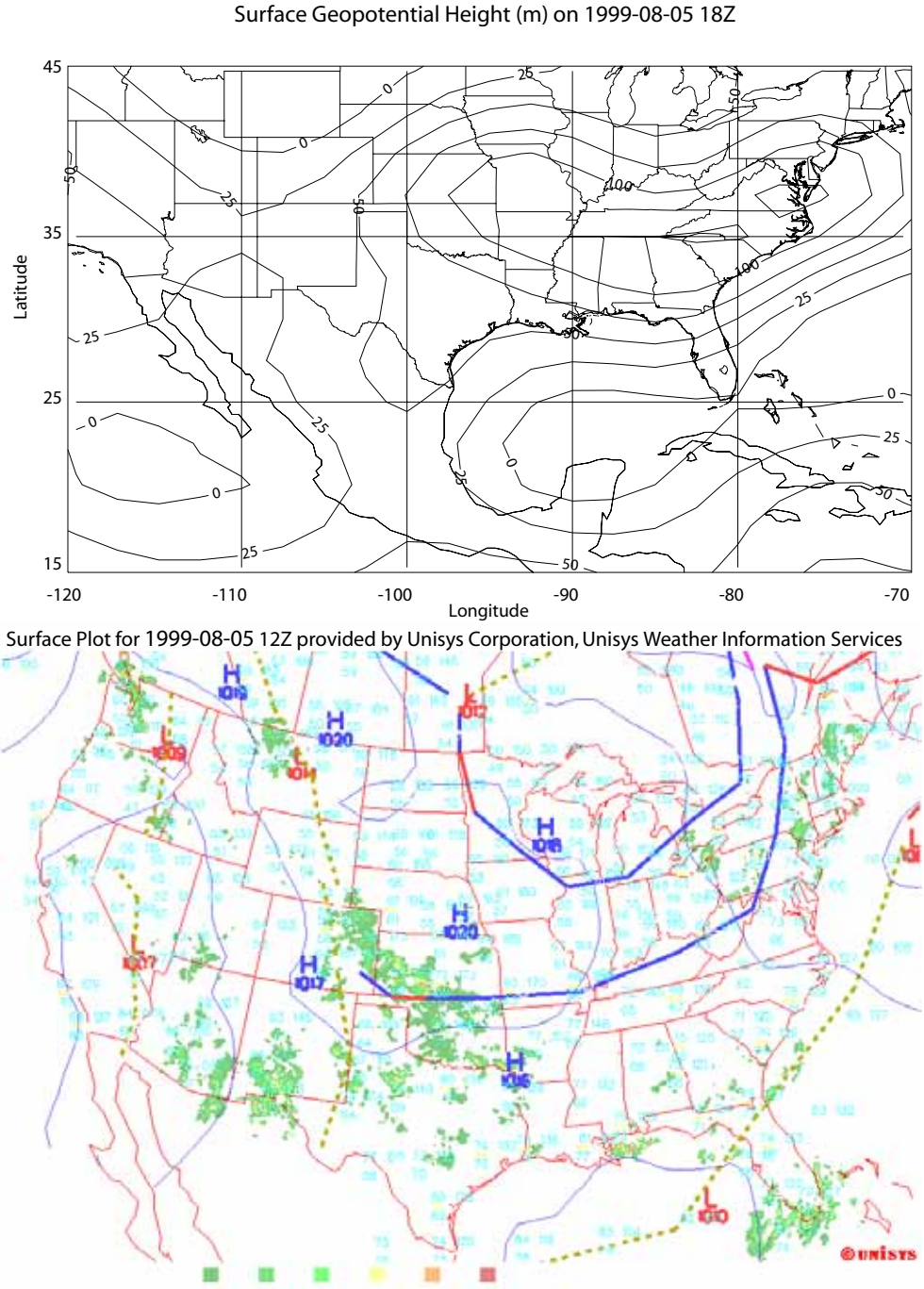

Fig. 32. Geopotential height in m at 1000 hPa on 1999-08-05 at 18Z and a plot of surface weather on 1999-08-05 at 12Z provided by Unisys Corporation, Unisys Weather Information Services..

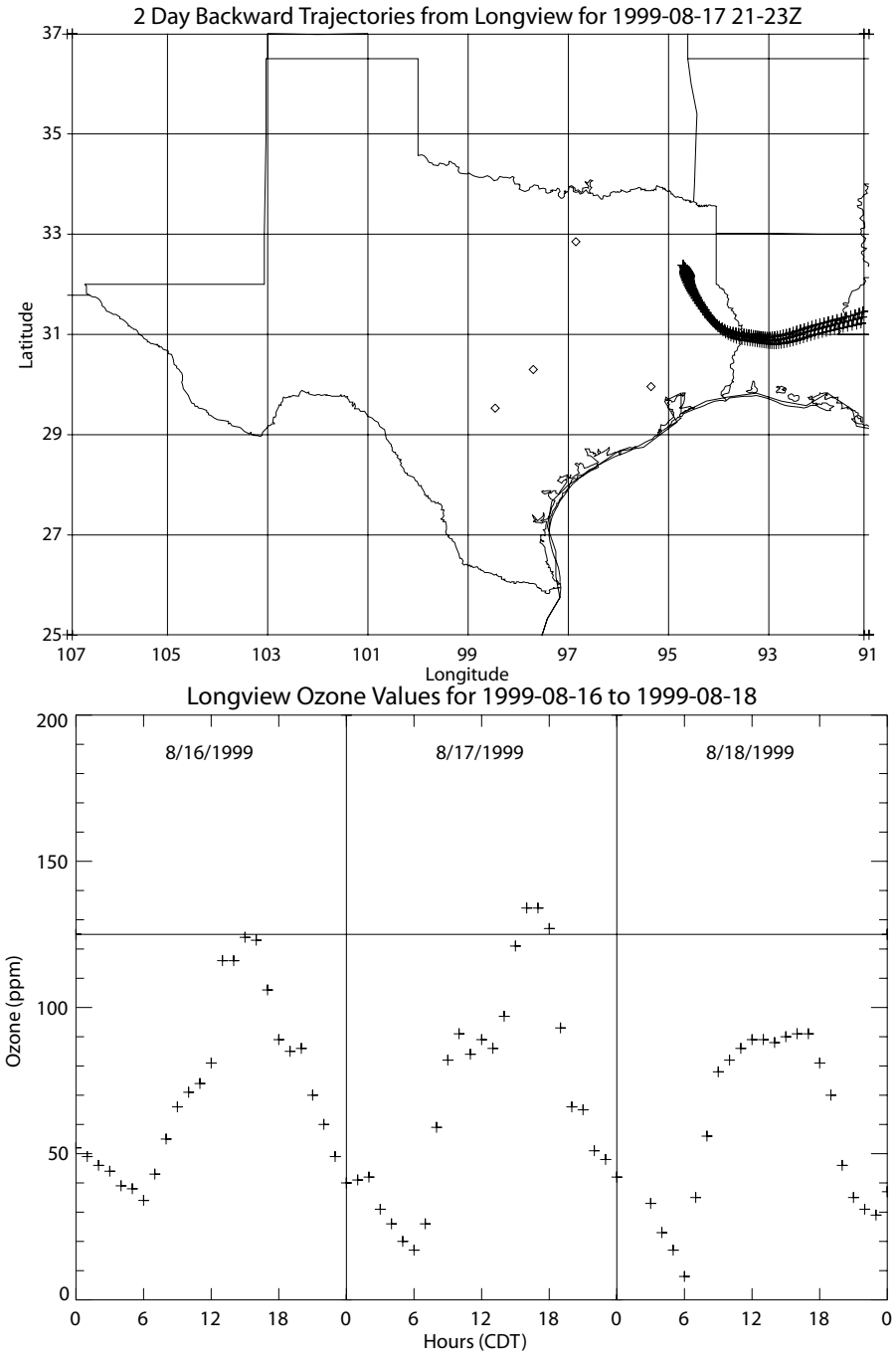

Fig. 33. 48-hour backward trajectories from Longview C19 for Event 12. Ozone values for 1999-08-16–1999-08-18 are also shown.

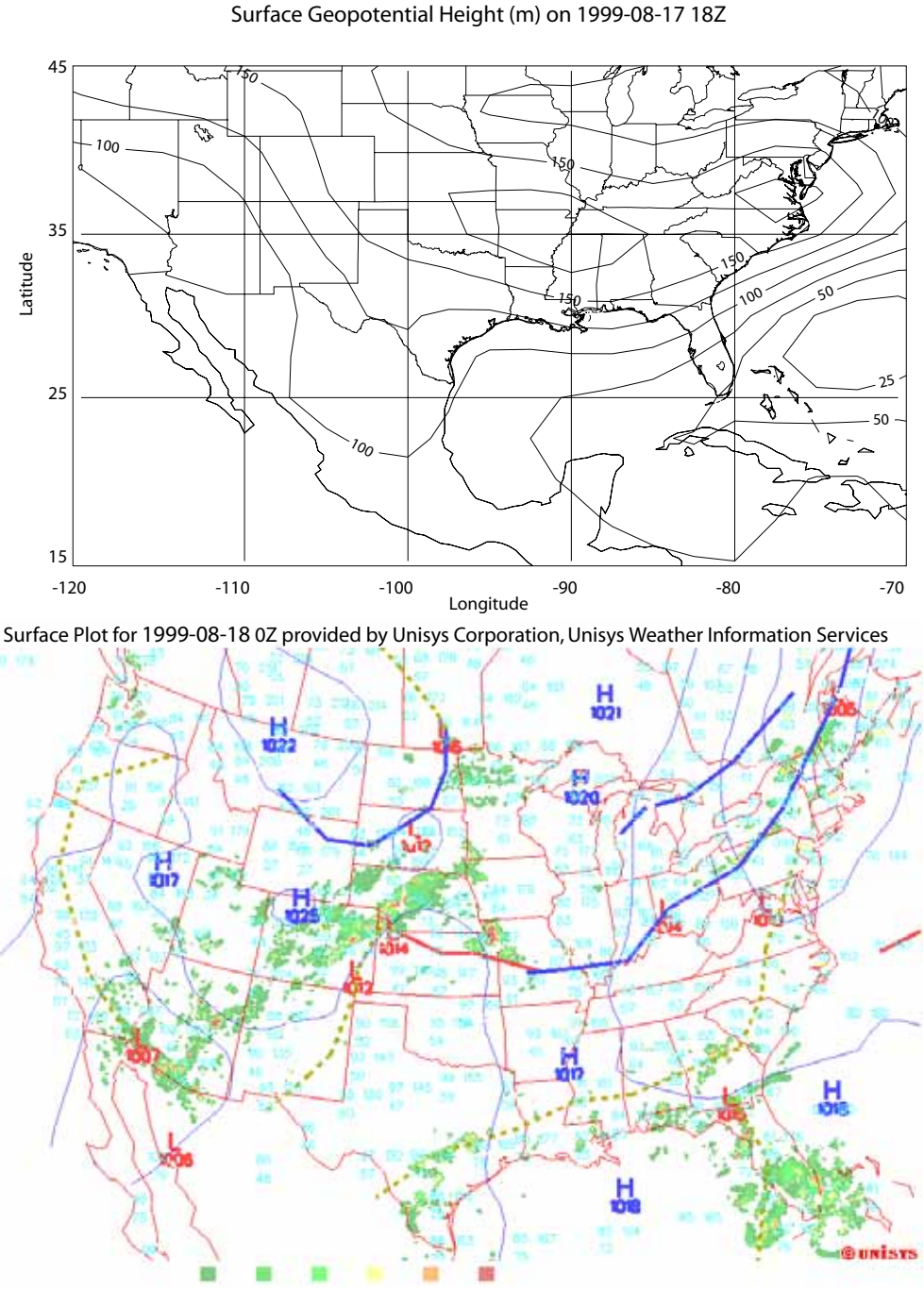

Fig. 34. Geopotential height in m at 1000 hPa on 1999-08-17 at 18Z and a plot of surface weather on 1999-08-18 at 0Z provided by Unisys Corporation, Unisys Weather Information Services.

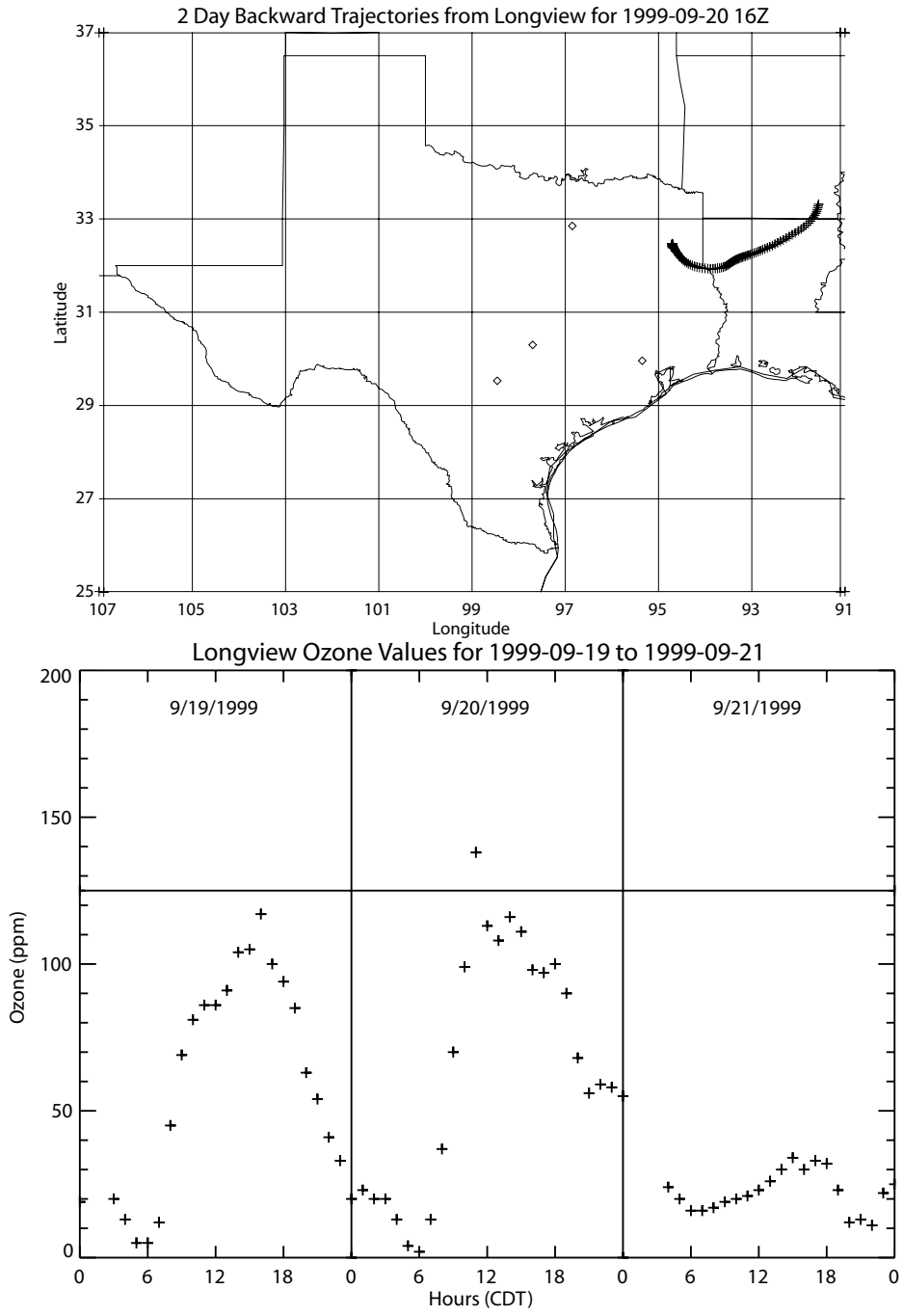

Fig. 35. 48-hour backward trajectory for Event 13. Ozone values for 1999-09-19–1999-09-21 are also shown.

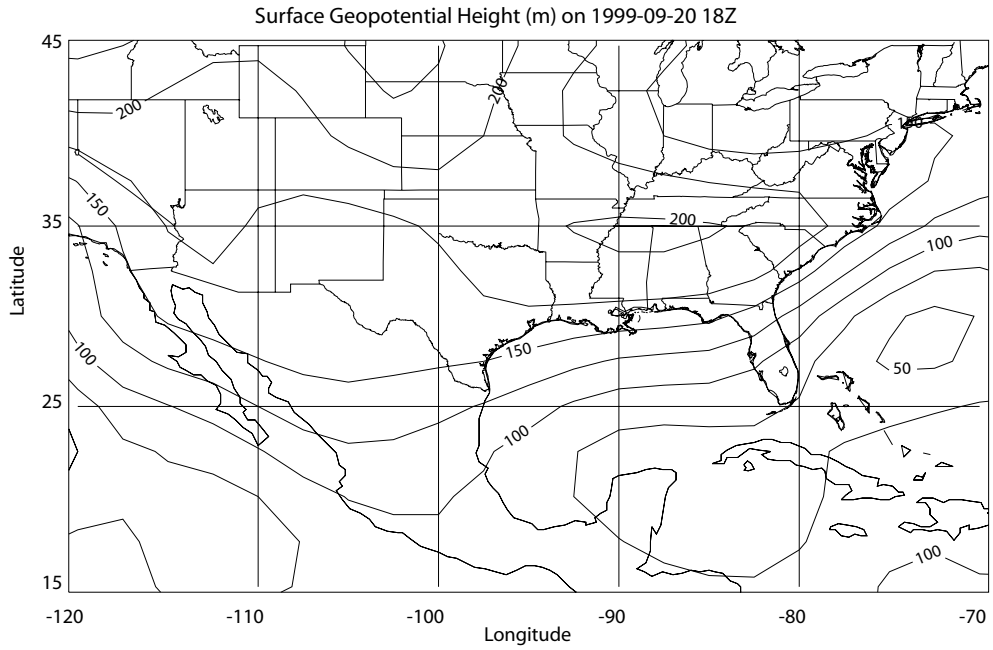

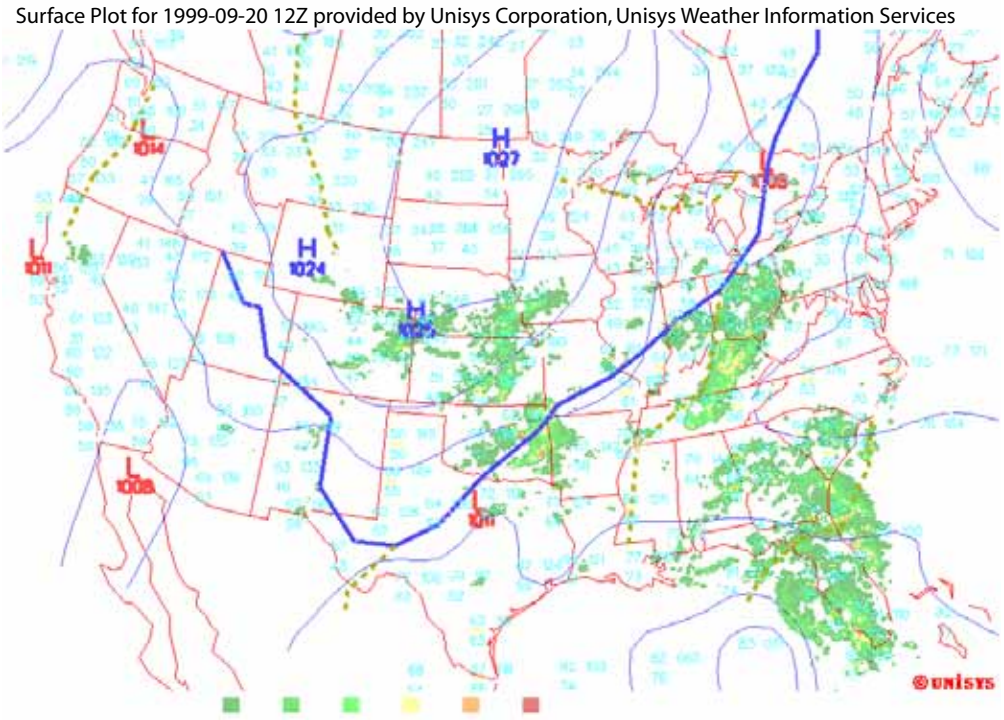

Fig. 36. Geopotential height in m at 1000 hPa on 1999-09-20 at 18Z and a plot of surface weather on 91999-09-20 at 12Z provided by Unisys Corporation, Unisys Weather Information Services.

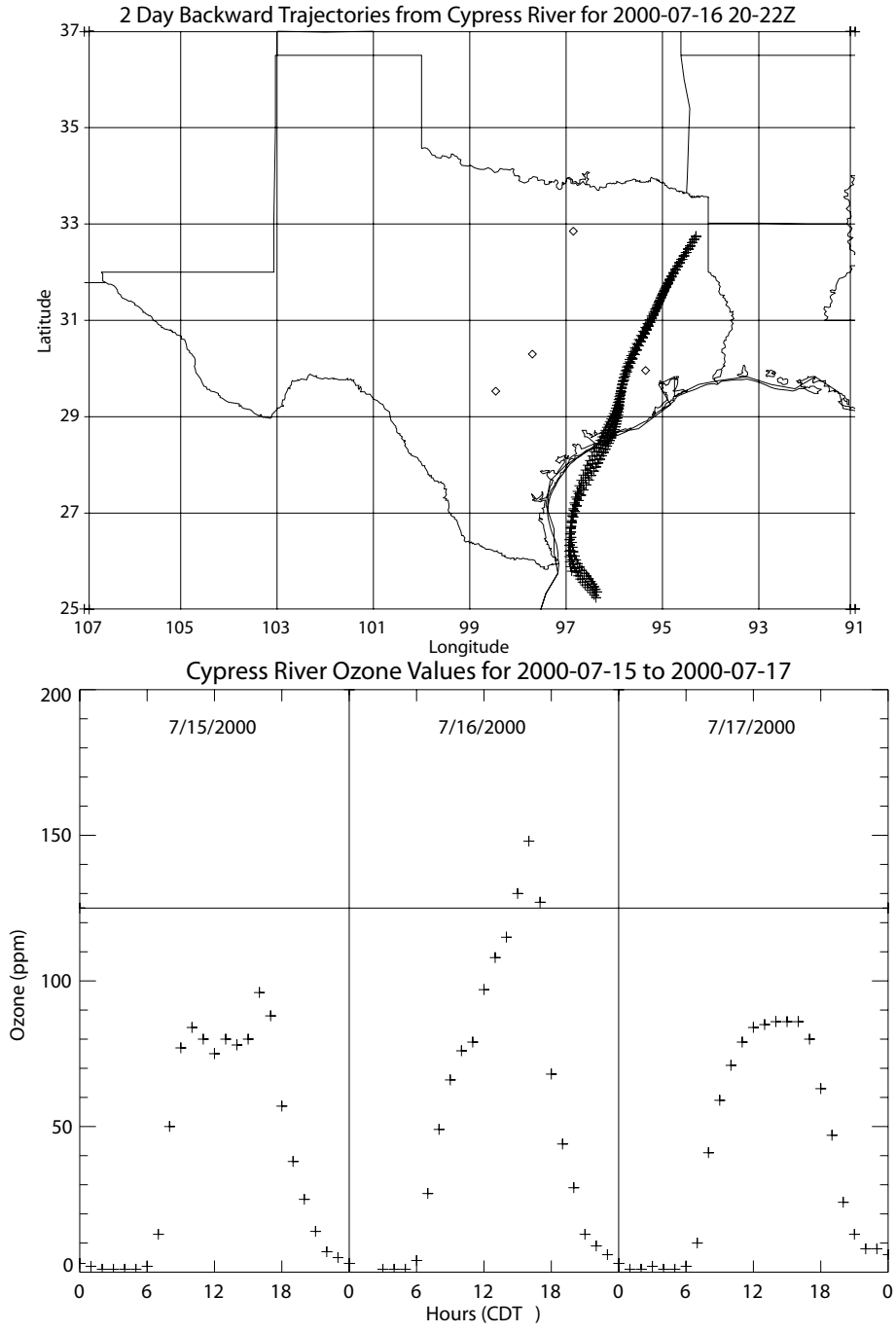

Fig. 37. 48-hour backward trajectories for Event 14. Ozone values for 2000-07-15–2000-07-17 are also shown.

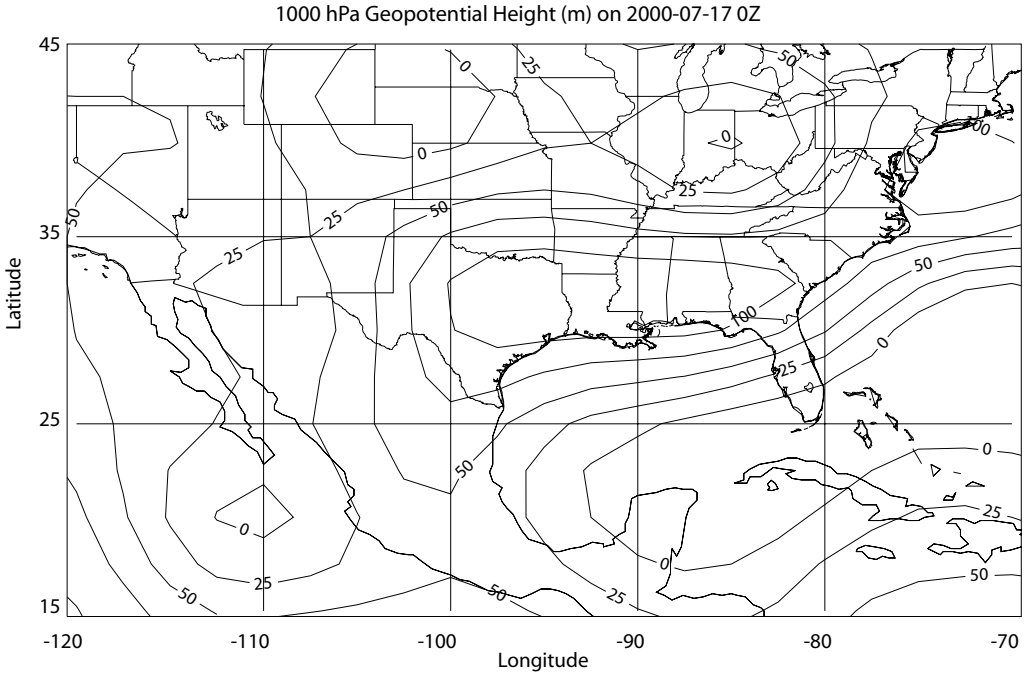

Fig. 38. Geopotential height in m at 1000 hPa on 2000-07-17 at 0Z and a plot of surface weather on 2000-07-16 at 0Z provided by Unisys Corporation, Unisys Weather Information Services.

CHAPTER V

CONCLUSIONS

A. Conclusions from Green's function methods

During the summer season the atmospheric circulation over Texas is dominated by the clockwise circulation around the Bermuda High. Trajectories calculated using kinematic Lagrangian methods show that air throughout most of Texas moves north before gradually curving east as a consequence of the clockwise circulation. Accordingly, particles released in Houston move first north and then east, following trajectories through east and northeast Texas over the 24-hour period following release. By estimating Green's functions for the transport equation from the trajectories, it is possible to evaluate the probable evolution of an arbitrary initial distribution of a trace substance. The calculated Green's functions can be applied to questions of urban air quality, such as when and to what extent pollution from a given source impacts another area.

B. Conclusions from CAMS Lagrangian trajectories

The percentage of trajectories approaching the sites Tyler Airport C86, Longview C19, and Fort Worth Northwest C13 in July and August from the north and east increases with increasing ozone value. The percentages of high and exceedance level trajectories approaching from the north and east are larger than the percentage of total trajectories that approach from the north and east for the three sites as well. These two relationships indicate that transport from the north and east is associated with increased ozone values.

The polluted air arriving at the CAMS sites from the east and northeast could have acquired its pollutant load along the Gulf Coast and in the southeast U.S. or possibly from

farther north in the midwest. Further study will be necessary to distinguish between these alternatives.

The majority of trajectories from Cypress River C50 come from the left side of the line despite ozone value. However, too much value should not be imparted to this result due to the small sample size of high and exceedance-level ozone values at the station. The majority of trajectories for all four groups in September 1996-1999 from Aldine C8 and Longview C19 come from the north and east, or the right side of the line, due to the increase in the frequency of frontal passages with the onset of fall.

C. Conclusions from synoptic method

It appears that the relatively high pressure associated with the Bermuda High that typically causes calm winds, clear skies, and southerly flow over Texas in the summer is not sufficient on its own to produce an ozone exceedance. Only one exceedance of those discussed here was produced under those conditions, that being the exceedance that occurred in Longview on August 16, 1998. Of the remaining exceedances 62% were associated with the passage of a cold front, while 38% were associated with the passage of a trough.

It appears that the passage of fronts and troughs is conducive to exceedances because of the transport of air from the southeast or midwest parts of the U.S. into Texas. Northeasterly flow could also bring ozone-laden air from the southeast into the region. Additionally, high pressure develops in the wake of these passages, causing conditions favorable to ozone exceedances such as clear skies, calm winds, and high temperatures.

The only southerly exceedance trajectory was Event 14 at Cypress River C50. The air was likely influenced by ozone precursors from metropolitan Houston on its way northeast,

and the exceedance was likely brought on by intrastate transport of ozone-laden air coupled with meteorological conditions favorable to an exceedance. Events 1–3 at Longview C19 all exhibited highly stagnant trajectories and comparatively low exceedance-level ozone values. These exceedance events can also likely be attributed to intrastate ozone-laden air transport coupled with meteorological conditions favorable to exceedances.

The remainder of the events' trajectories are either entirely northeasterly or largely northeasterly before making a clockwise turn to become southeasterly. Longview C19, Tyler Airport C86, and Fort Worth NW C13 experienced entirely northeasterly trajectories. Longview C19 and Aldine C08 experienced northeasterly rotating to southeasterly trajectories. Of the two trajectory types, the northeasterly rotating to southeasterly trajectories occurred with higher ozone values at Longview C19.

In conclusion, 28% of the exceedance trajectories can be attributed to intrastate transport while 72% undergo a significant amount of interstate travel. All of the interstate exceedance trajectories are from the northeast when initialized, 48 hours before arrival. This indicates a relationship between exceedance level ozone values in Texas and transport of air from states to the east and northeast.

REFERENCES

Bowman, K. P., and Carrie, G. D. 2002. The mean-meridional transport circulation of the troposphere in an idealized GCM. *J. Atmos. Sci.*, **59**, 1502–1514.

Hall, T. M., and Plumb, R. A. 1994. Age as a diagnostic of stratospheric transport. *J. Geophys. Res.*, **99**, 1059–1070.

Holzer, M. 1999. Analysis of passive tracer transport as modeled by an atmospheric general circulation model. *J. Climate*, **12**, 1659–1684.

Holzer, M., and Boer, G. J. 2000. Simulated changes in atmospheric transport climate. *J. Climate*, **14**, 4398–4420.

Kalnay, E., Kanamitsu, M., Kistler, R., Collins, W., and Deaven D., et al. 1996. The NCEP/NCAR 40-year reanalysis project. *Bull. Am. Meteorol. Soc.*, **77**, 437–471.

Peppler, R.A. 2000. ARM Southern Great Plains Site Observations of the Smoke Pall Associated with the 1998 Central American Fires. *Bull. Am. Meteorol. Soc.*, **81**, 2563–2591.

Rogers, C. M., and Bowman, K. P. 2001. Transport of smoke from the Central American fires of 1998. *J. Geophys. Res.*, **106**, 28,357–28,368.

Senff, C., Banta, R. M., Darby, L. S., R. J. Alvarez, II, and Sandberg S. P., et al. 2002. Horizontal and vertical distribution of ozone in the Houston area during the 8/29/2000-9/6/2000 pollution episode. Report 10.18: available from American Meteorological Society in Boston, MA.

Texas Commission on Environmental Quality in Austin, Texas. 2000. State Implementation Plan for ozone in Texas, Appendix N: Demonstration of transport from the HGA ozone nonattainment area to DFW. April 2000 revision.

VITA

Darielle Nicole Dexheimer attended The University of Texas at Austin from 1996–2000 with a major in hydrogeology. She attended Texas A&M University in May 2000 and received her Bachelor of Science in atmospheric sciences in 2001. In May 2001 she began graduate school at Texas A&M University on a UNESCO fellowship. Ms. Dexheimer can be reached through her parents at 720 Carol Ln., Burleson, Texas.

The research for this thesis was supported by a two and a half year grant from the Texas Air Research Center. The grant was intended to support investigation into regional-scale atmospheric transport and air quality in Texas.